NATIONAL ADVISORY COMMITTEE FOR AERONAUTICS

REPORT 1012

INVESTIGATION OF THE NACA 4-(5)(08)-03 AND NACA 4-(10)(08)-03 TWO-BLADE PROPELLERS AT FORWARD MACH NUMBERS TO 0.725 TO DETERMINE THE EFFECTS OF CAMBER AND COMPRESSIBILITY ON PERFORMANCE

By JAMES B. DELANO



1951

For sale by the Superintendent of Documents, U. S. Government Printing Office, Washington 25, D. C. Yearly subscription, $4.00; foreign, $5.25; single copy price varies according to size. - - - - - - - - - Price 30 cents

AERONAUTIC SYMBOLS

1. FUNDAMENTAL AND DERIVED UNITS

	Symbol	Metric		English	
		Unit	Abbreviation	Unit	Abbreviation
Length	l	meter	m	foot (or mile)	ft (or mi)
Time	t	second	s	second (or hour)	sec (or hr)
Force	F	weight of 1 kilogram	kg	weight of 1 pound	lb
Power	P	horsepower (metric)		horsepower	hp
Speed	V	kilometers per hour	kph	miles per hour	mph
		meters per second	mps	feet per second	fps

2. GENERAL SYMBOLS

W Weight $=mg$

g Standard acceleration of gravity $=9.80665$ m/s^2 or 32.1740 ft/sec^2

m Mass $=\frac{W}{g}$

I Moment of inertia $=mk^2$. (Indicate axis of radius of gyration k by proper subscript.)

μ Coefficient of viscosity

ν Kinematic viscosity

ρ Density (mass per unit volume)

Standard density of dry air, 0.12497 kg-m^{-4}-s^2 at 15° C and 760 mm; or 0.002378 lb-ft^{-4} sec^2

Specific weight of "standard" air, 1.2255 kg/m^3 or 0.07651 lb/cu ft

3. AERODYNAMIC SYMBOLS

S Area

S_w Area of wing

G Gap

b Span

c Chord

A Aspect ratio, $\frac{b^2}{S}$

V True air speed

q Dynamic pressure, $\frac{1}{2}\rho V^2$

L Lift, absolute coefficient $C_L=\frac{L}{qS}$

D Drag, absolute coefficient $C_D=\frac{D}{qS}$

D_0 Profile drag, absolute coefficient $C_{D_0}=\frac{D_0}{qS}$

D_i Induced drag, absolute coefficient $C_{D_i}=\frac{D_i}{qS}$

D_p Parasite drag, absolute coefficient $C_{D_p}=\frac{D_p}{qS}$

C Cross-wind force, absolute coefficient $C_C=\frac{C}{qS}$

i_w Angle of setting of wings (relative to thrust line)

i_t Angle of stabilizer setting (relative to thrust line)

Q Resultant moment

Ω Resultant angular velocity

R Reynolds number, $\rho\frac{Vl}{\mu}$ where l is a linear dimension (e.g., for an airfoil of 1.0 ft chord, 100 mph, standard pressure at 15° C, the corresponding Reynolds number is 935,400; or for an airfoil of 1.0 m chord, 100 mps, the corresponding Reynolds number is 6,865,000)

α Angle of attack

ϵ Angle of downwash

α_0 Angle of attack, infinite aspect ratio

α_i Angle of attack, induced

α_a Angle of attack, absolute (measured from zero-lift position)

γ Flight-path angle

REPORT 1012

INVESTIGATION OF THE NACA 4-(5)(08)-03 AND NACA 4-(10)(08)-03 TWO-BLADE PROPELLERS AT FORWARD MACH NUMBERS TO 0.725 TO DETERMINE THE EFFECTS OF CAMBER AND COMPRESSIBILITY ON PERFORMANCE

By JAMES B. DELANO

Langley Aeronautical Laboratory
Langley Field, Va.

National Advisory Committee for Aeronautics

Headquarters, 1724 F Street NW., Washington 25, D. C.

Created by act of Congress approved March 3, 1915, for the supervision and direction of the scientific study of the problems of flight (U. S. Code, title 50, sec. 151). Its membership was increased from 12 to 15 by act approved March 2, 1929, and to 17 by act approved May 25, 1948. The members are appointed by the President, and serve as such without compensation.

JEROME C. HUNSAKER, Sc. D., Massachusetts Institute of Technology, *Chairman*

ALEXANDER WETMORE, Sc. D., Secretary, Smithsonian Institution, *Vice Chairman*

DETLEV W. BRONK, PH. D., President, Johns Hopkins University.

JOHN H. CASSADY, Vice Admiral, United States Navy, Deputy Chief of Naval Operations.

EDWARD U. CONDON, PH. D., Director, National Bureau of Standards.

HON. THOMAS W. S. DAVIS, Assistant Secretary of Commerce.

JAMES H. DOOLITTLE, Sc. D., Vice President, Shell Union Oil Corp.

R. M. HAZEN, B. S., Director of Engineering, Allison Division, General Motors Corp.

WILLIAM LITTLEWOOD, M. E., Vice President, Engineering, American Airlines, Inc.

THEODORE C. LONNQUEST, Rear Admiral, United States Navy, Deputy and Assistant Chief of the Bureau of Aeronautics.

DONALD L. PUTT, Major General, United States Air Force, Director of Research and Development, Office of the Chief of Staff, Matériel.

ARTHUR E. RAYMOND, Sc. D., Vice President, Engineering, Douglas Aircraft Co., Inc.

FRANCIS W. REICHELDERFER, Sc. D., Chief, United States Weather Bureau.

HON. DELOS W. RENTZEL, Administrator of Civil Aeronautics, Department of Commerce.

GORDON P. SAVILLE, Major General, United States Air Force, Deputy Chief of Staff—Development.

WILLIAM WEBSTER, M. S., Chairman, Research and Development Board, Department of Defense.

THEODORE P. WRIGHT, Sc. D., Vice President for Research Cornell University.

HUGH L. DRYDEN, PH. D., *Director*

JOHN W. CROWLEY, JR., B. S., *Associate Director for Research*

JOHN F. VICTORY, LL. D., *Executive Secretary*

E. H. CHAMBERLIN, *Executive Officer*

HENRY J. E. REID, D. Eng., Director, Langley Aeronautical Laboratory, Langley Field, Va.

SMITH J. DEFRANCE, B. S., Director, Ames Aeronautical Laboratory, Moffett Field, Calif.

EDWARD R. SHARP, Sc. D., Director, Lewis Flight Propulsion Laboratory, Cleveland Airport, Cleveland, Ohio

TECHNICAL COMMITTEES

AERODYNAMICS
POWER PLANTS FOR AIRCRAFT
AIRCRAFT CONSTRUCTION
OPERATING PROBLEMS
INDUSTRY CONSULTING

Coordination of Research Needs of Military and Civil Aviation
Preparation of Research Programs
Allocation of Problems
Prevention of Duplication
Consideration of Inventions

LANGLEY AERONAUTICAL LABORATORY, Langley Field, Va.

LEWIS FLIGHT PROPULSION LABORATORY, Cleveland Airport, Cleveland, Ohio

AMES AERONAUTICAL LABORATORY, Moffett Field, Calif.

Conduct, under unified control, for all agencies, of scientific research on the fundamental problems of flight

OFFICE OF AERONAUTICAL INTELLIGENCE,
Washington, D. C.

Collection, classification, compilation, and dissemination of scientific and technical information on aeronautics

REPORT 1012

INVESTIGATION OF THE NACA 4–(5)(08)–03 AND NACA 4–(10)(08)–03 TWO-BLADE PROPELLERS AT FORWARD MACH NUMBERS TO 0.725 TO DETERMINE THE EFFECTS OF CAMBER AND COMPRESSIBILITY ON PERFORMANCE [1]

By James B. Delano

SUMMARY

As part of a general investigation of propellers at high forward speeds, tests of two-blade propellers having the NACA 4–(5)(08)–03 and NACA 4–(10)(08)–03 blade designs were made in the Langley 8-foot high-speed tunnel through a range of blade angle from 20° to 60° for forward Mach numbers from 0.165 to 0.70 to determine the effect of camber and compressibility on propeller characteristics. Results previously reported for similar tests of a two-blade propeller having the NACA 4–(3)(08)–03 blade design are included for comparison.

Blades of high design camber were more efficient than blades of low design camber for operation at high power loadings. The blade of highest camber gave efficiencies 15 to 25 percent higher than the efficiencies of the low-camber and medium-camber blades for high power loadings at advance ratios corresponding to take-off and climb at low Mach numbers. The NACA 4–(5)(08)–03 propeller generally gave peak efficiencies 2 to 5 percent higher than those for the NACA 4–(3)(08)–03 propeller and 3 to approximately 12 percent higher than those for the NACA 4–(10)(08)–03 propeller. These higher efficiencies were due mainly to reduced compressibility losses. At the design blade angle of 45°, the critical tip Mach number for maximum efficiency was 0.01 higher for the NACA 4–(5)(08)–03 propeller than for the NACA 4–(3)(08)–03 propeller, which began to show compressibility losses at a tip Mach number of approximately 0.90. The NACA 4–(10)(08)–03 propeller began to show compressibility losses at a tip Mach number as low as 0.70 but, because of the large power-absorbing capacity of this propeller, produced about 46 percent more thrust than the NACA 4–(5)(08)–03 propeller for a high-speed operating condition corresponding to a tip Mach number of 0.86, a forward Mach number of 0.53, and an advance ratio of 2.48.

INTRODUCTION

Many airplanes now take off and climb with propellers at least partly stalled, and the tendency to use increasing powers may aggravate a condition that is already serious. Flight at high altitudes also may necessitate propeller operation at high lift coefficients, which would increase possible stall and compressibility effects and result in a reduction of propeller efficiency.

The National Advisory Committee for Aeronautics has attempted to improve propeller performance by conducting a general investigation of propellers at high forward speeds. This investigation included the effects on propeller characteristics of compressibility, blade solidity, and blade-section camber. The research program included tests of propellers of a sufficient range of blade forms to make possible the study of changes in blade shapes that might be required as a consequence of compressibility effects.

The effects of compressibility and solidity on performance as determined from tests of the NACA 4–(3)(08)–03 and NACA 4–(3)(08)–045 two-blade propellers (reference 1) constituted the initial phase of a general investigation of propellers at high forward speeds. The effects of camber and compressibility on performance as determined from tests of the NACA 4–(5)(08)–03 and NACA 4–(10)(08)–03 two-blade propellers constituted the second phase of the investigation and are presented herein. These results are compared with results of reference 1, for the NACA 4–(3)(08)–03 propeller, in order to indicate the effects of section design camber for propellers operating over a wide range of forward Mach number. These three blade designs cover the practical range of blade section camber.

SYMBOLS

B	number of blades
b	blade width, feet
b/D	blade width ratio
c_d	blade-section profile-drag coefficient
c_l	blade-section lift coefficient
c_{l_d}	blade-section design lift coefficient
C_P	power coefficient $\left(\frac{P}{\rho n^3 D^5}\right)$
C_T	thrust coefficient $\left(\frac{T}{\rho n^2 D^4}\right)$
$C_{T_{max}}$	maximum thrust coefficient
D	propeller diameter, feet
G	Goldstein tip-correction factor
h	maximum thickness of blade section, feet
h/b	blade thickness ratio
J	advance ratio (V_0/nD)
M	tunnel-datum (forward) Mach number (tunnel-empty Mach number uncorrected for tunnel-wall constraint)
M_t	helical tip Mach number $\left(M\sqrt{1+\left(\frac{\pi}{J}\right)^2}\right)$
n	propeller rotational speed, revolutions per second
P	power absorbed by the propeller, foot-pounds per second

[1] Supersedes NACA ACR L5F15, "Investigation of Two-Blade Propellers at High Forward Speeds in the NACA 8-Foot High-Speed Tunnel. III—Effects of Camber and Compressibility NACA 4–(5)(08)–03 and NACA 4–(10)(08)–03 Blades" by James B. Delano, 1945.

P_c power disk-loading coefficient $\left(\frac{P}{\frac{1}{2}\rho V_0^3 S}\right)$

R propeller tip radius, feet

r blade-section radius, feet

S propeller disk area, square feet $\left(\frac{\pi D^2}{4}\right)$

T propulsive thrust of propeller, pounds

T_c thrust disk-loading coefficient $\left(\frac{T}{\rho V^2 D^2}\right)$

V tunnel-datum velocity (tunnel-empty velocity uncorrected for tunnel-wall constraint), feet per second

V_0 equivalent free-air velocity (tunnel-datum velocity corrected for tunnel-wall constraint), feet per second

r/R blade-section station

α_i induced angle of attack, degrees $\left(\tan^{-1}\frac{\sigma c_l}{4G\sin\phi}\right)$

β section blade angle, degrees

$\beta_{0.75R}$ section blade angle at 0.75 tip radius, degrees

$\gamma=\tan^{-1}\frac{c_d}{c_l}$, degrees

η propulsive efficiency $\left(\frac{C_T}{C_P}J\right)$

η_{max} maximum propulsive efficiency

ρ air density, slugs per cubic foot

σ total blade-section solidity $(Bb/2\pi r)$

ϕ aerodynamic helix angle, degrees $(\phi_0+\alpha_i)$

ϕ_0 geometric helix angle, degrees $\left(\tan^{-1}\frac{JR}{\pi r}\right)$

APPARATUS, METHODS, AND TESTS

The apparatus and methods described in reference 1 were used in the present investigation. The investigation was conducted in the Langley 8-foot high-speed tunnel. A photograph showing the model setup is given as figure 1.

The blades of the propellers investigated were designed for three-blade propellers to produce minimum induced energy losses (profile drag assumed equal to zero) at a blade angle of approximately 45° at the 0.7-radius station. The blade sections are late-critical-speed sections of the NACA 16 series (reference 2); methods and principles employed in the design of the blades are discussed in reference 3. The blades differ only in design camber and are designated as NACA 4–(3)(08)–03 (low camber, reference 1), NACA 4–(5)(08)–03 (medium camber), and NACA 4–(10)(08)–03(high camber).

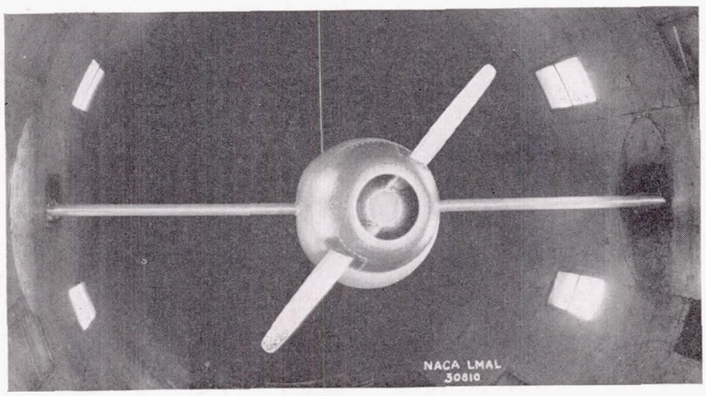


FIGURE 1.—Setup for testing propellers in the Langley 8-foot high-speed tunnel.

The designation numbers describe the propellers. The number (or numbers) of the first group is the diameter in feet; the number (or numbers) of the second group (enclosed within the first set of parentheses) is the design lift coefficient (in tenths) of the blade section at the 0.7-radius station; the numbers of the third group (enclosed within the second set of parentheses) are the thickness ratio of the blade section at the 0.7-radius station; and the numbers of the fourth group are the blade solidity expressed as the ratio of the blade chord at the 0.7-radius station to the circumference of the circle having a radius 0.7 of the propeller tip radius. The NACA 4–(10)(08)–03 propeller thus has a diameter of 4 feet and the blade section at the 0.7-radius station has a design lift coefficient of 1.0, a thickness ratio of 0.08, and a blade solidity of 0.03.

Blade-form curves for the propellers are presented in figure 2. A photograph of one of these blades and a comparison of the sections at the 0.7-radius station are given as figure 3.

The range of this investigation was the same, within power limitations, as that of reference 1. The range of blade angle and tunnel-datum Mach number is given in table I.

REDUCTION OF DATA

The data have been reduced to the usual thrust and power coefficients and efficiency and have been corrected for the propulsive effects of the cowling and spinner and for tunnel-wall constraint. The tunnel-wall constraint necessitated a velocity correction to free-air conditions and a model-drag correction because of the buoyancy effect. The methods involved in making these corrections are discussed in reference 1.

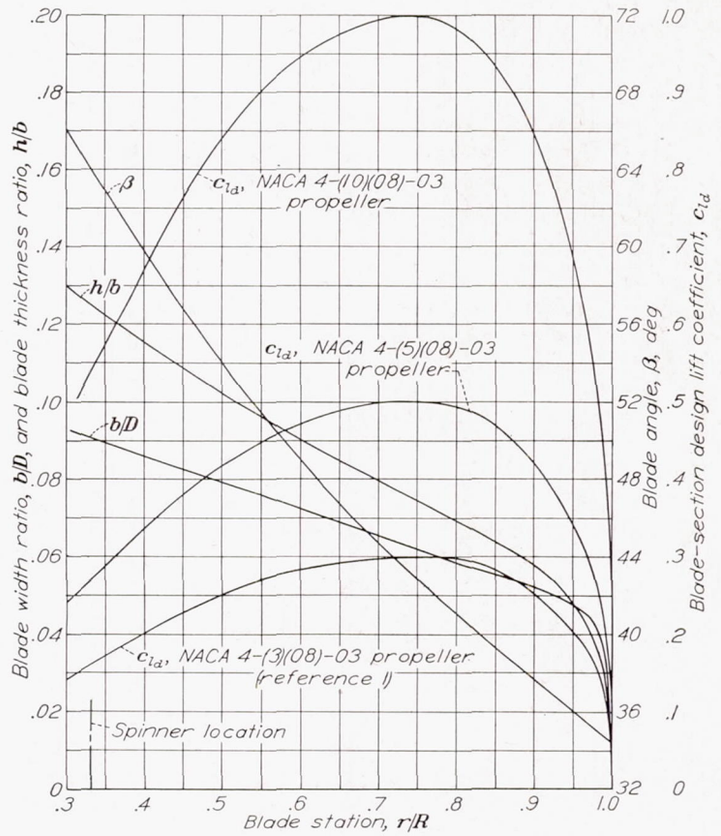
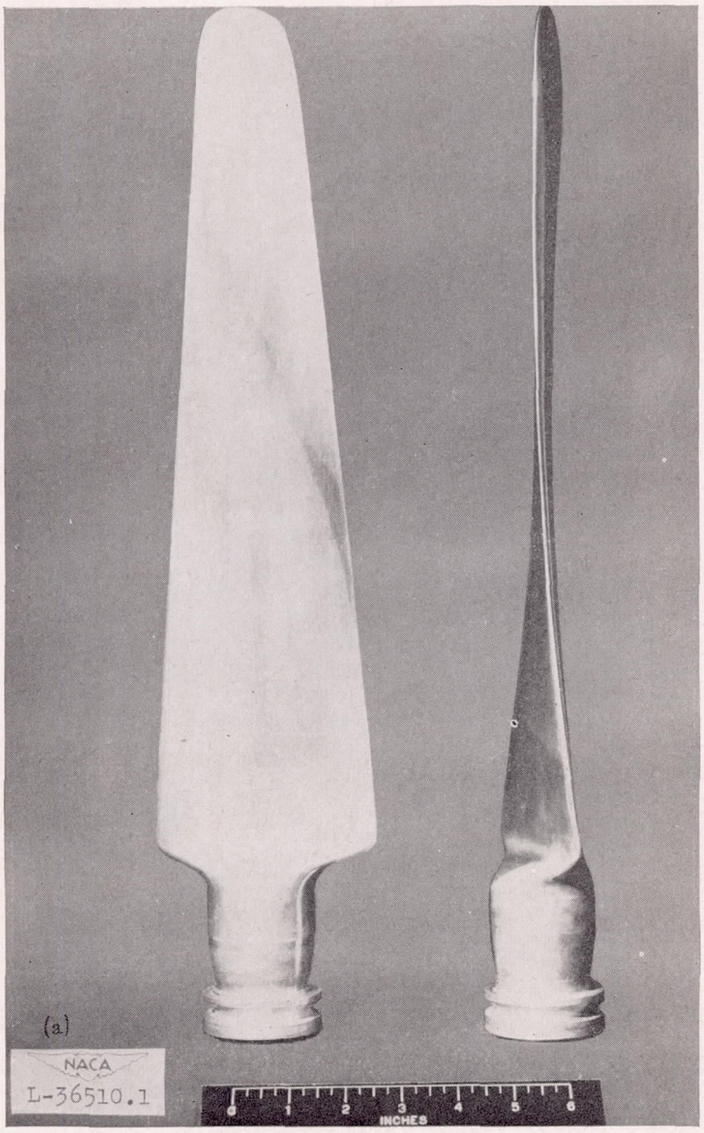


FIGURE 2.—Blade-form curves.



(a) Typical test blade.
(b) Sections at 0.7 radius.

FIGURE 3.—Typical test blade and comparison of sections at 0.7 radius.

Thrust.—The thrust coefficient was determined from the propulsive thrust, that is, the net measured force minus the drag of the model without the propeller and minus the thrust due to the buoyancy effect (see reference 1).

Velocity correction due to tunnel-wall constraint.—The equivalent free-stream velocity corresponding to the thrust and torque of the propeller measured at each rotational speed differs from the tunnel-datum velocity (tunnel empty) because of the flow constraint produced by the tunnel walls.

TABLE I.—TEST RANGE OF BLADE ANGLE AND MACH NUMBER

Tunnel-datum (forward) Mach number, M	Blade angle at 0.75 radius, $\beta_{0.75R}$ (deg)								
0.165	[a] 20	25	30	35	40	45	50	55	60
.23	[a] 20	25	30	35	40	45	50	55	60
.35		[b] 25	30	35	40	45	50	55	60
.43				35	40	45	50	55	60
.53					40	45	50	55	60
.60						45	50	55	60
.65							50	55	60
.675							50	55	60
.70							50	55	60
.725							50	55	60

[a] Except for NACA 4-(10)(08)-03 propeller.
[b] Except for NACA 4-(3)(08)-03 and NACA 4-(5)(08)-03 propellers.

The velocity correction, which has been applied to the calculation of advance ratio, is presented in figure 4 as the ratio of free-air velocity to the tunnel-datum velocity (tunnel empty) as a function of the thrust disk-loading coefficient. The tunnel-wall correction was found to be dependent only on the thrust disk-loading coefficient for the range of tunnel speed and propeller operation used in this investigation.

The tunnel-datum Mach number has not been corrected for tunnel-wall constraint. For the range of velocity shown in figure 4, the factors required to correct the tunnel-datum velocity and tunnel-datum Mach numbers to the free-stream condition are essentially equal.

RESULTS AND DISCUSSION

The basic characteristics for the NACA 4-(5)(08)-03 and NACA 4-(10)(08)-03 two-blade propellers are presented in figures 5 and 6, respectively. For each value of the tunnel-datum Mach number the propeller thrust coefficient, power coefficient, and efficiency are plotted against advance ratio. The variation of tip Mach number with advance ratio is also included. As used in this report, the tunnel-datum Mach number M is not corrected for the effects of tunnel-wall constraint. The free-stream Mach number can be obtained by applying the tunnel-wall corrections presented in figure 4 to the tunnel-datum Mach number. Similarly, the corrected tip Mach number can also be obtained.

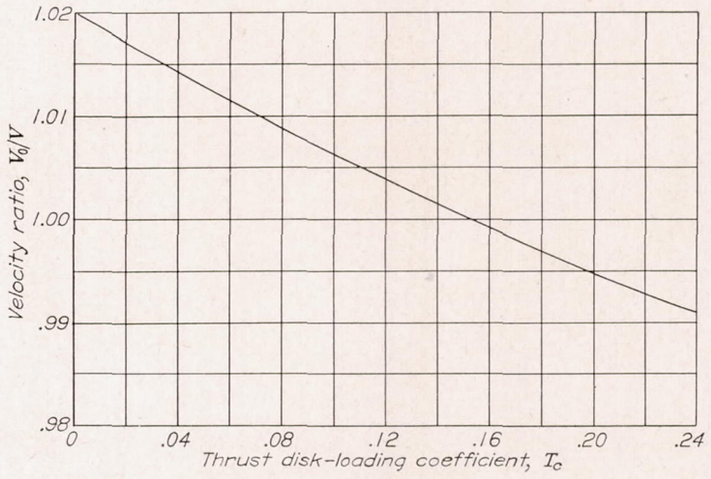
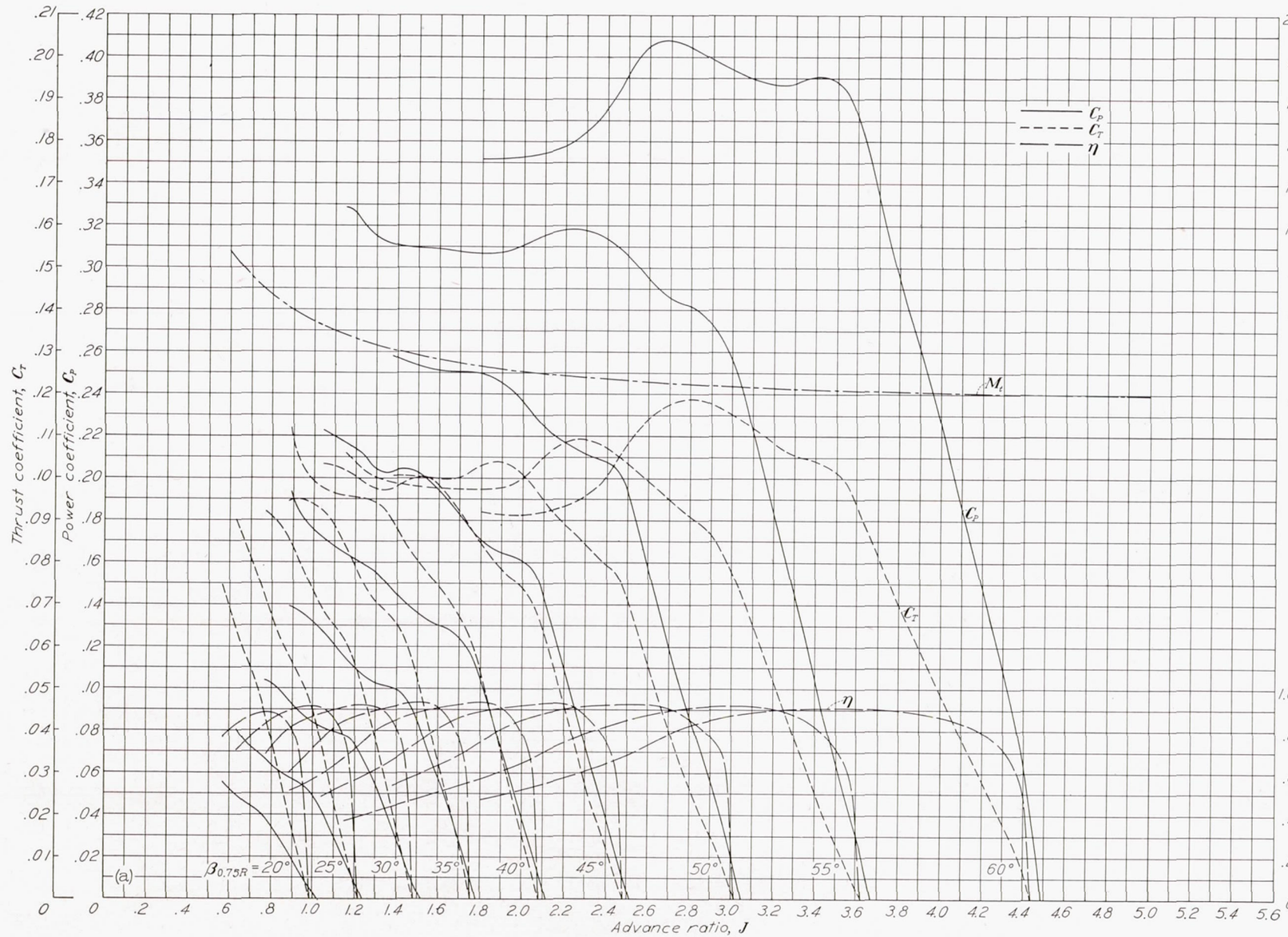
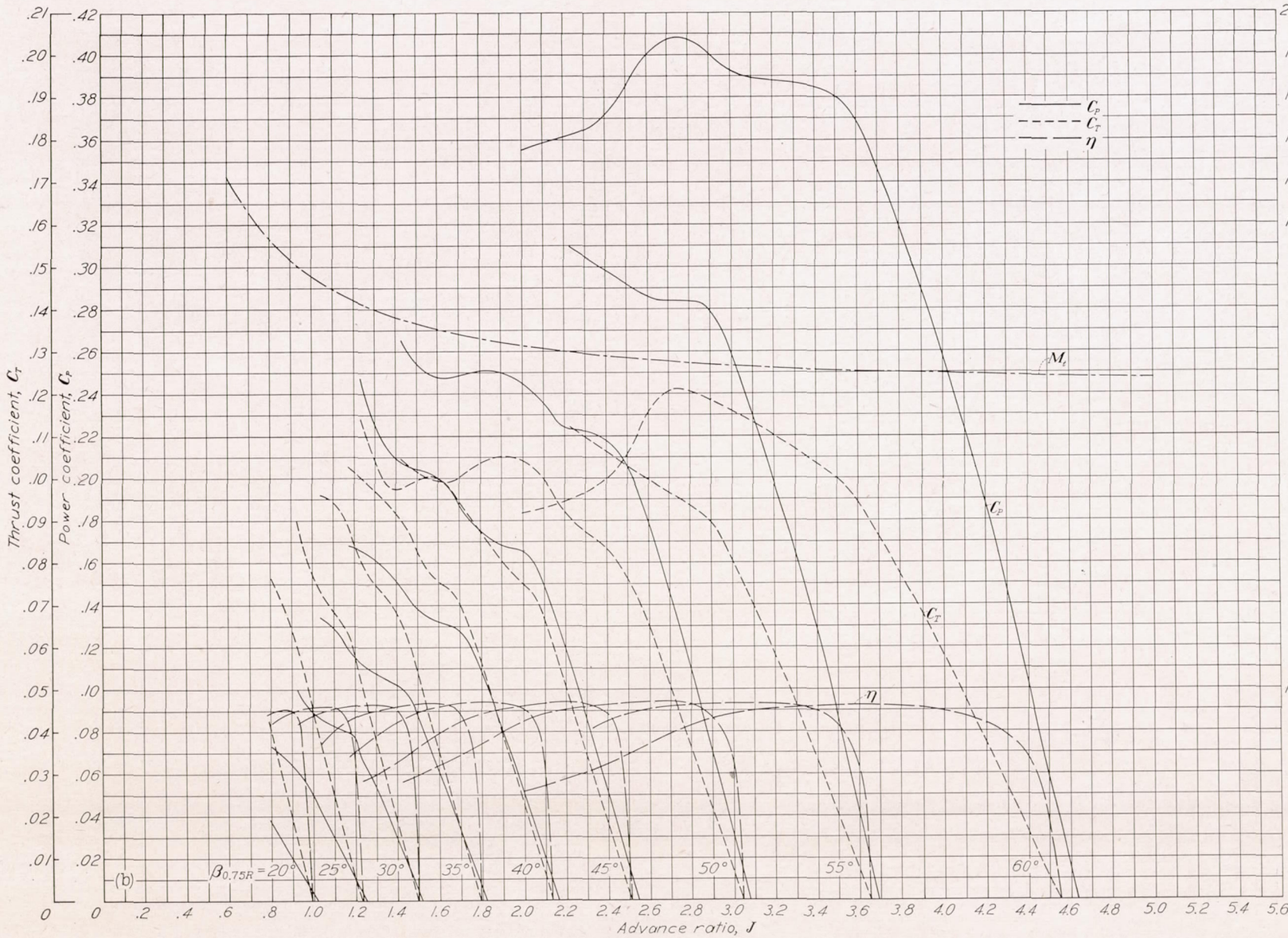


FIGURE 4.—Tunnel-wall interference correction.



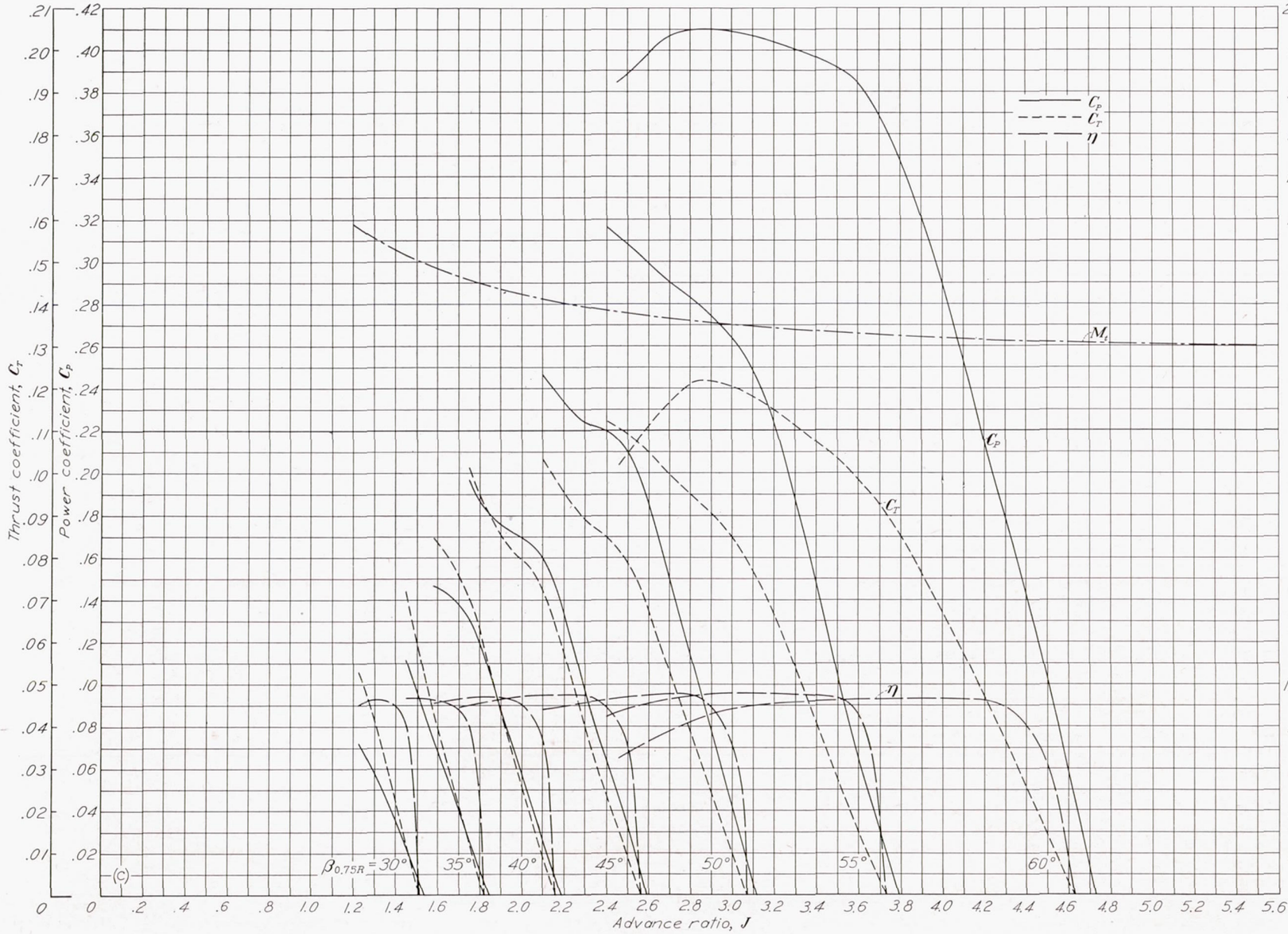
(a) $M=0.165$.

FIGURE 5.—Characteristics for the NACA 4-(5)(08)-03 propeller.



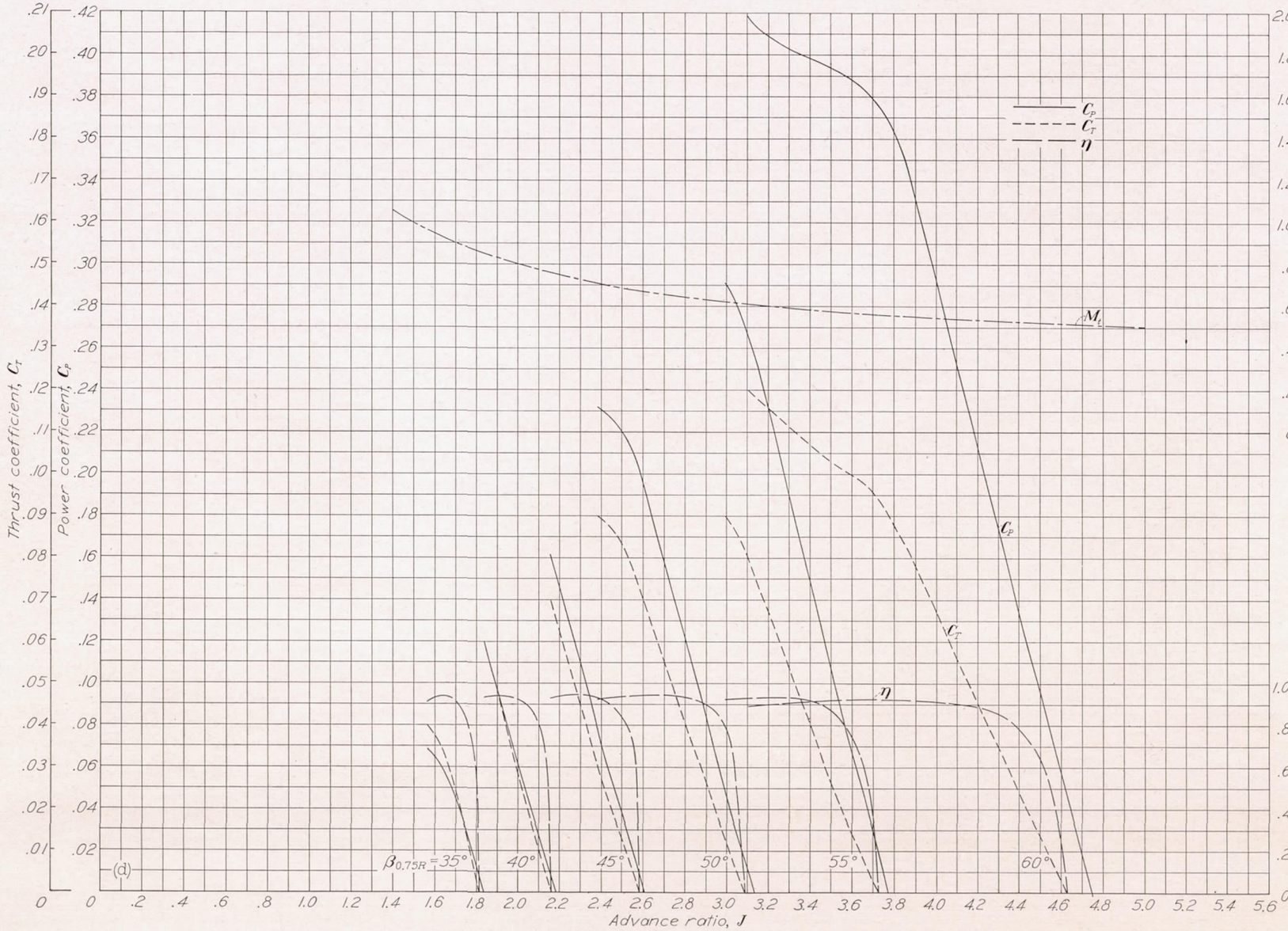
(b) M=0.23.

FIGURE 5.—Continued.



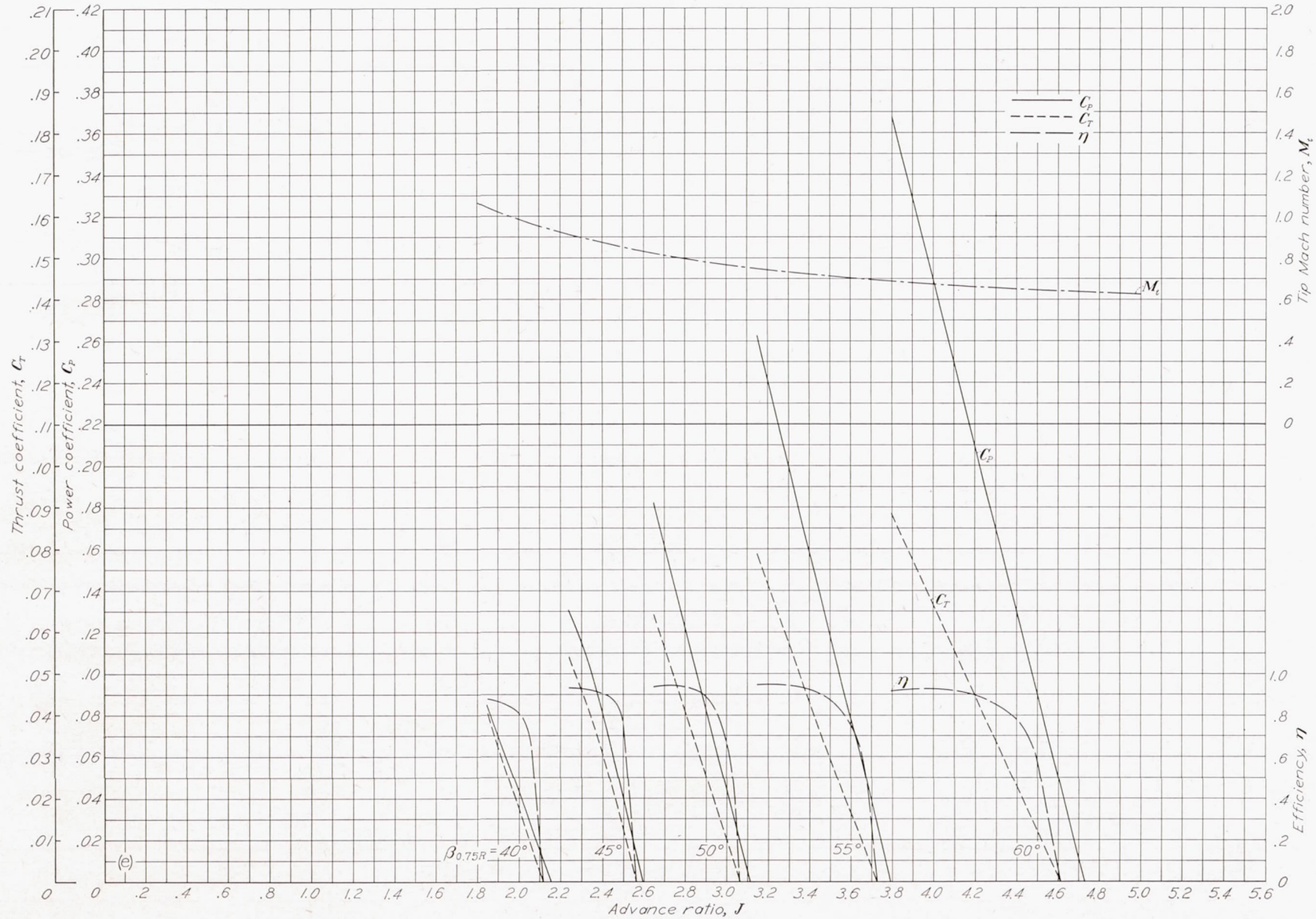
(c) $M=0.35$.

FIGURE 5.—Continued.



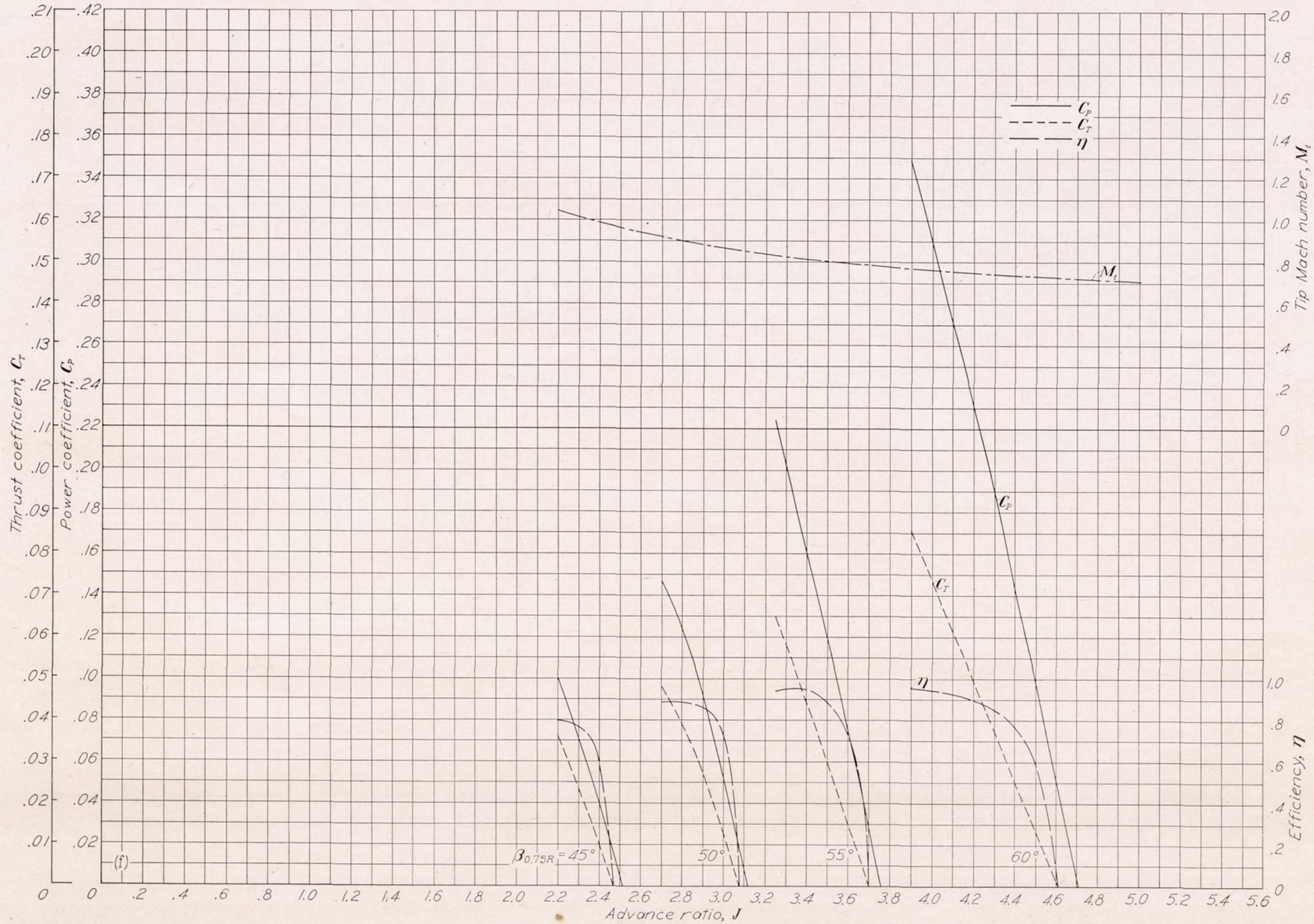
(d) M=0.43.

FIGURE 5.—Continued.



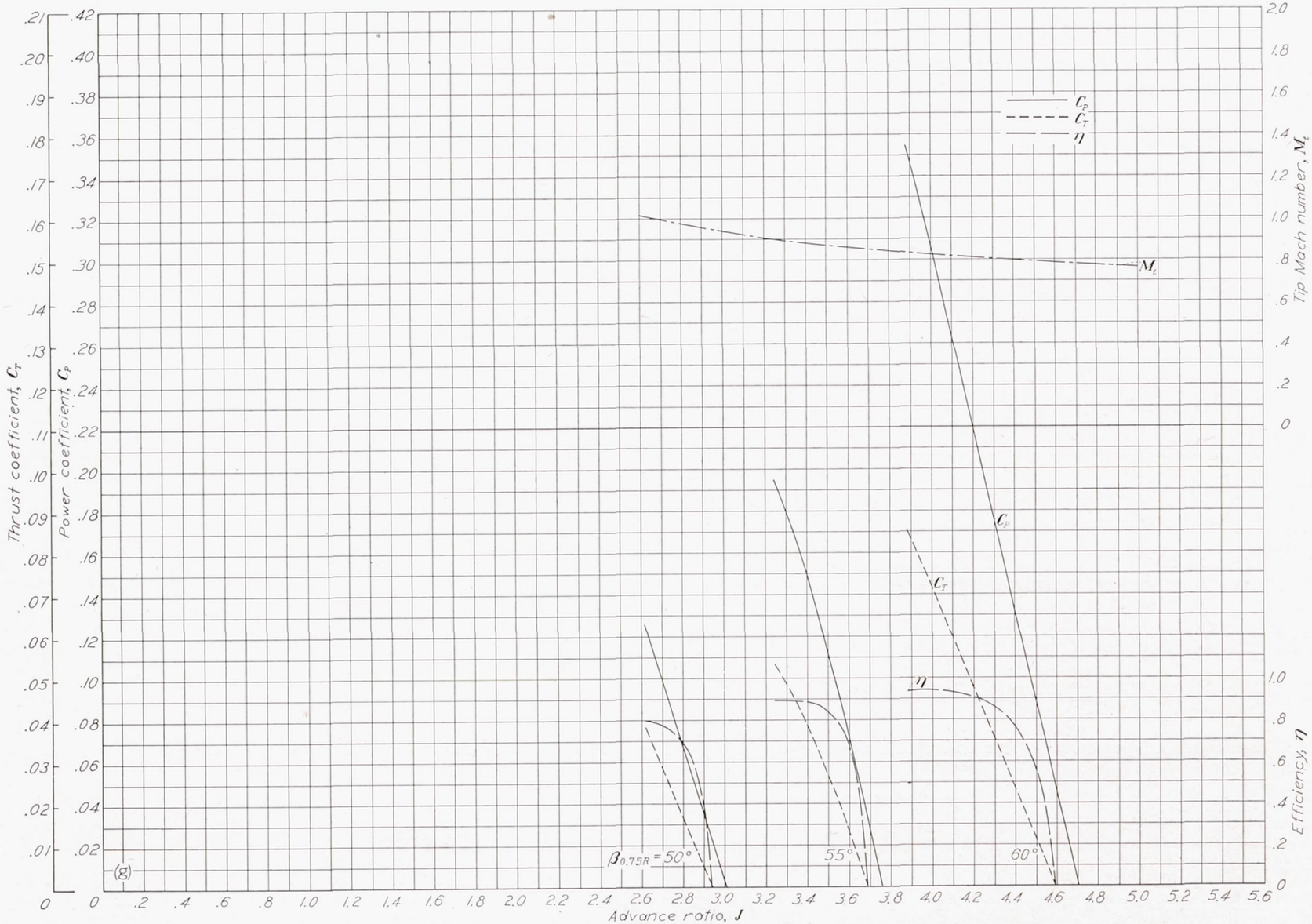
(e) M=0.53.

FIGURE 5.—Continued.



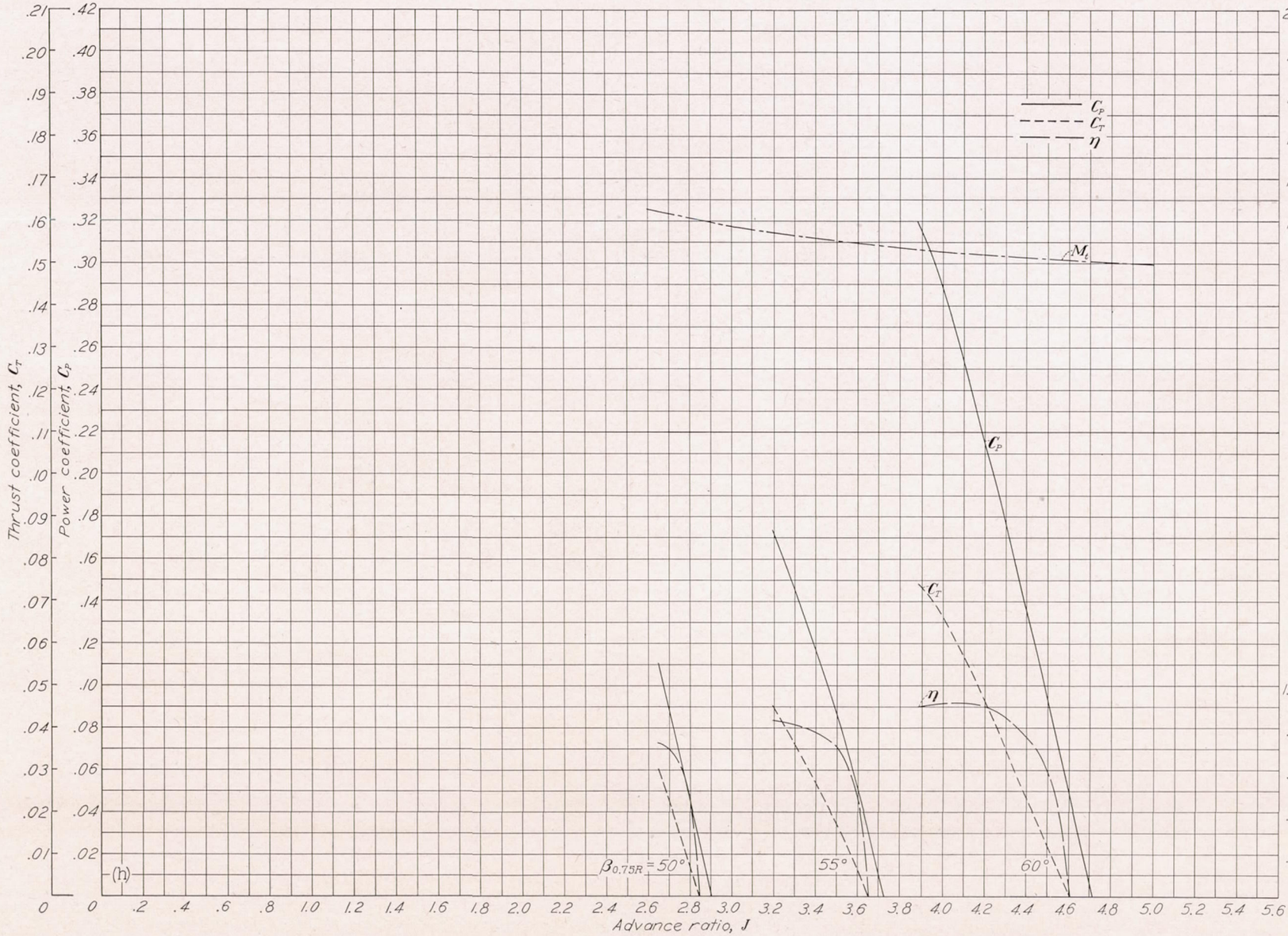
(f) M=0.60.

FIGURE 5.—Continued.



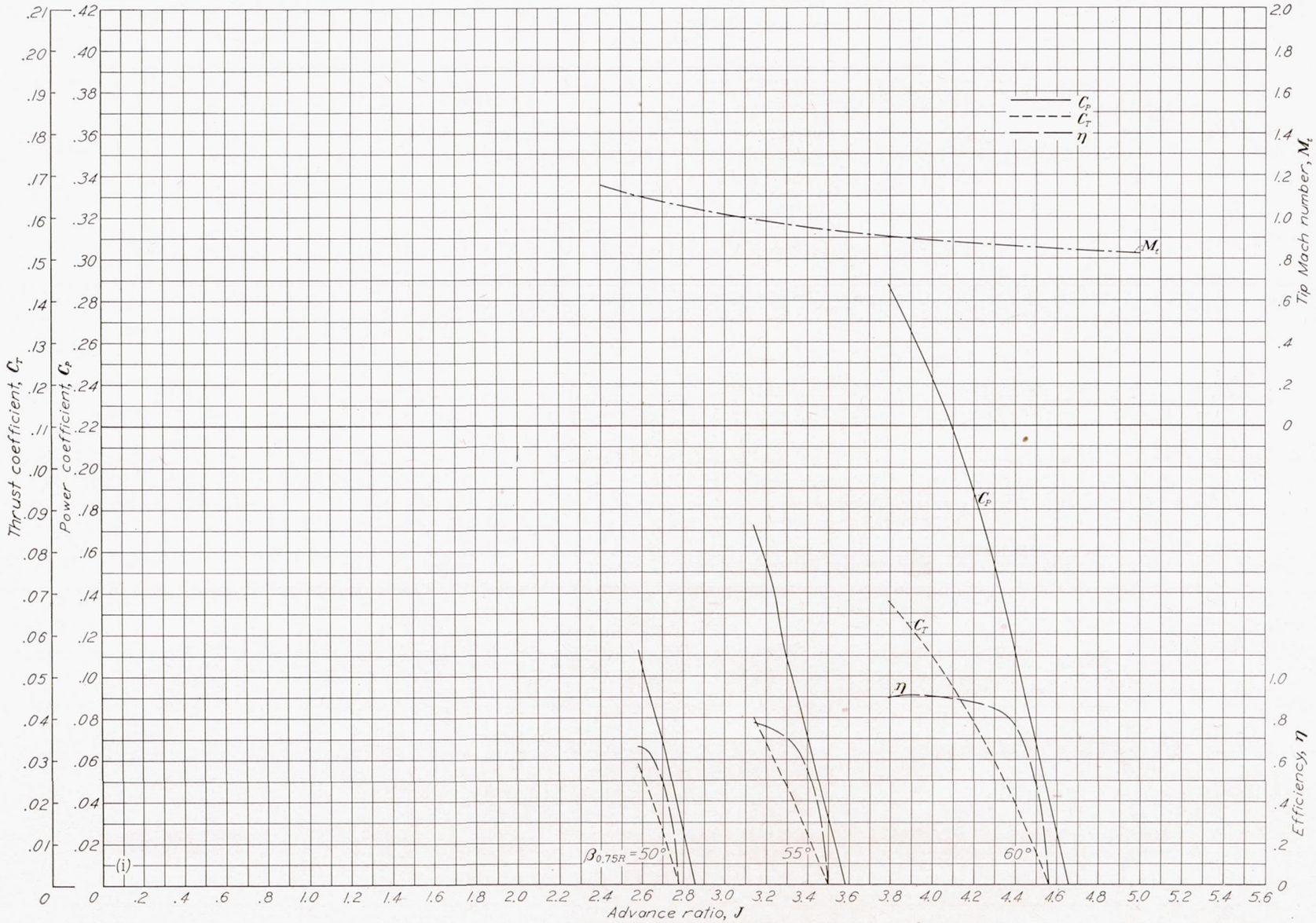
(g) $M=0.65$.

FIGURE 5.—Continued.



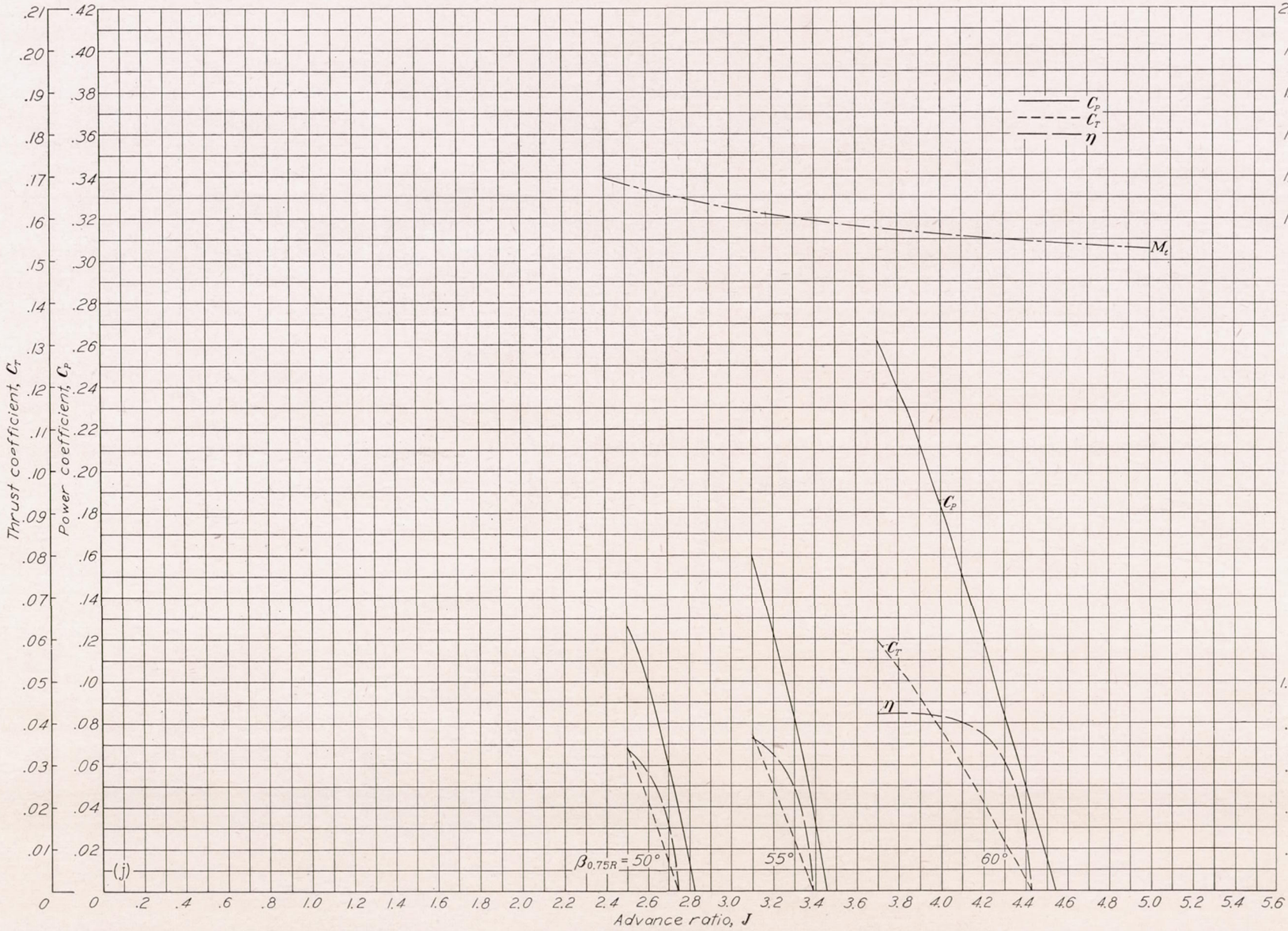
(h) $M=0.675$.

FIGURE 5.—Continued.



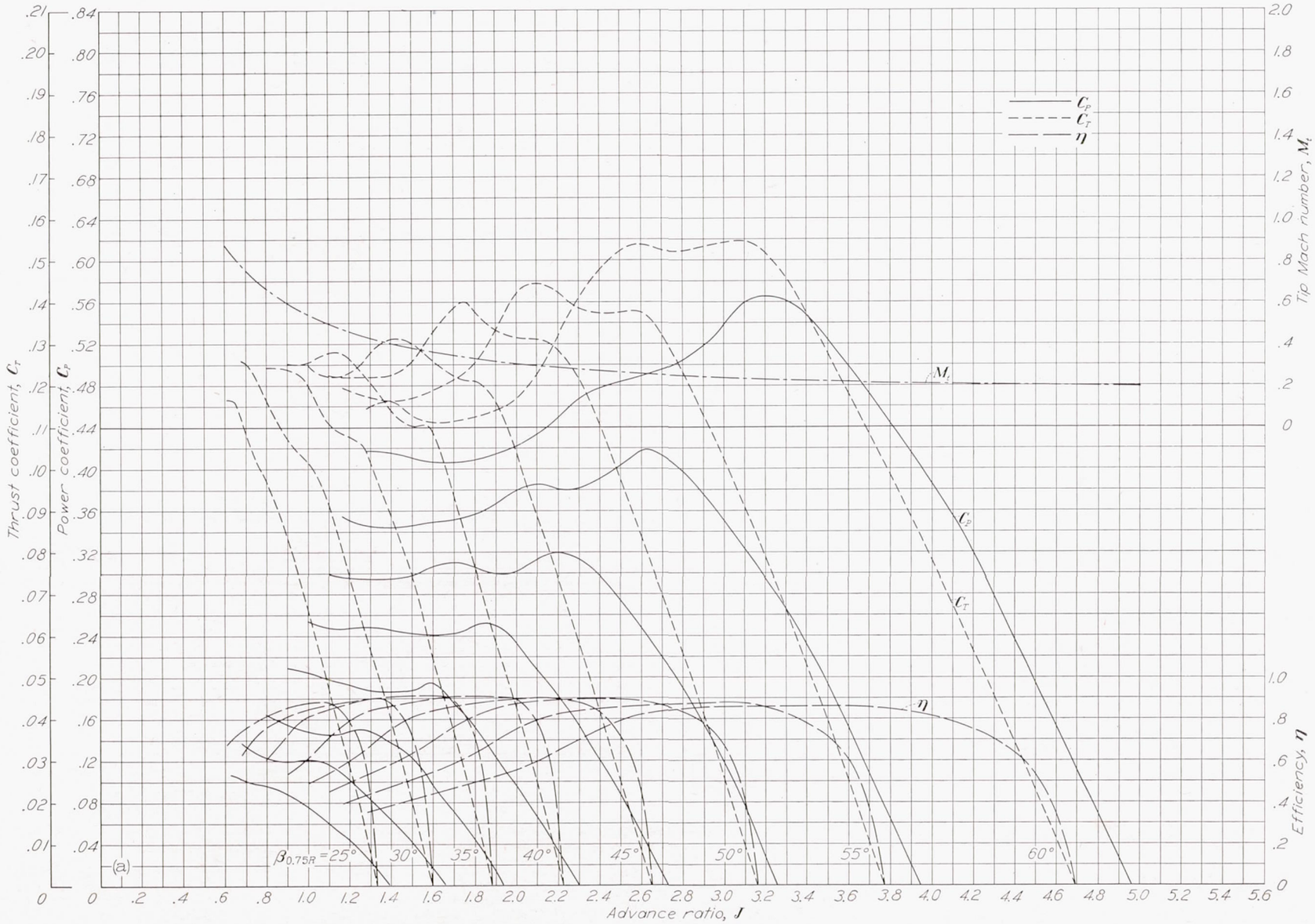
(i) M=0.70.

FIGURE 5.—Continued.



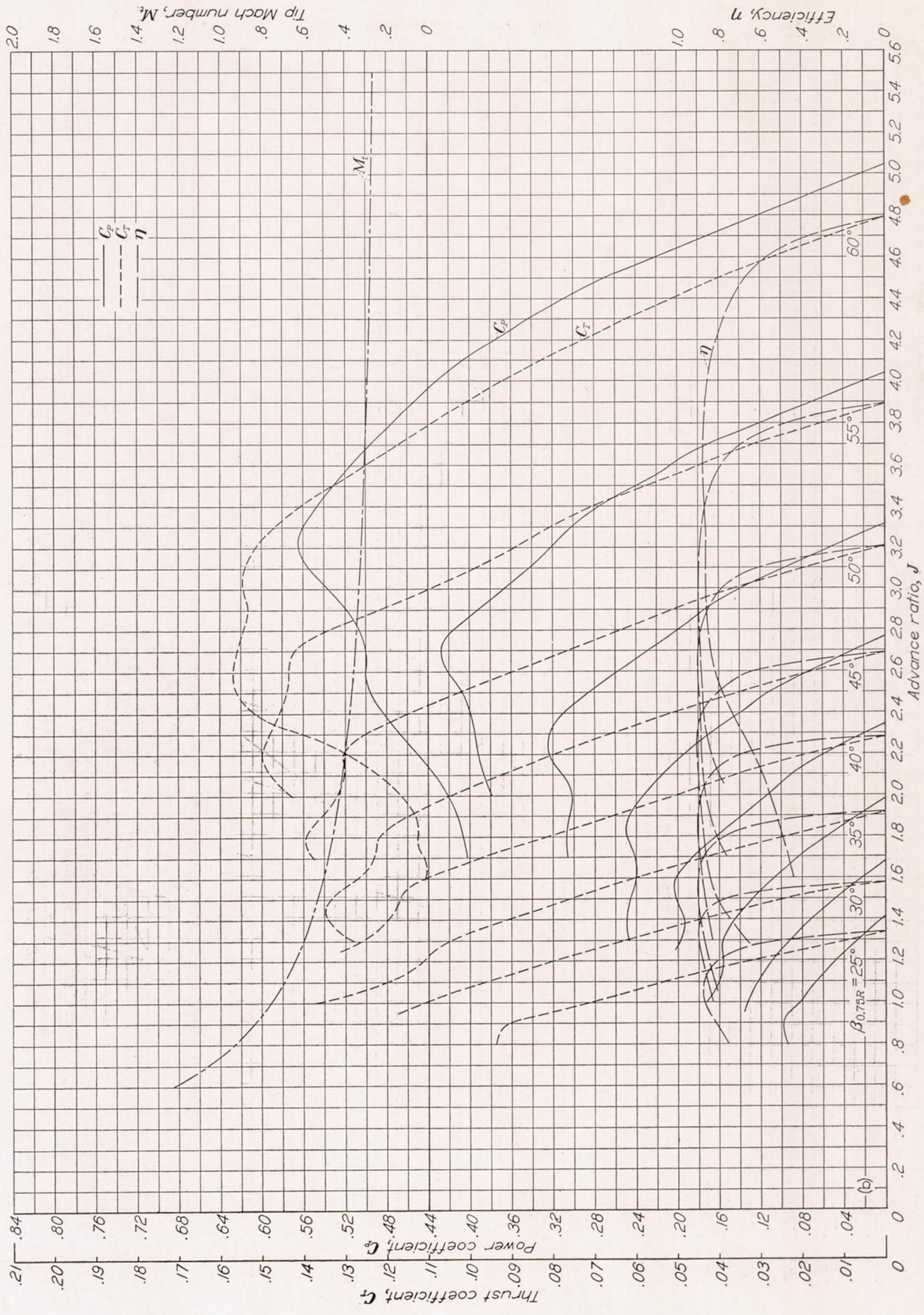
(j) $M=0.725$.

FIGURE 5.—Concluded.



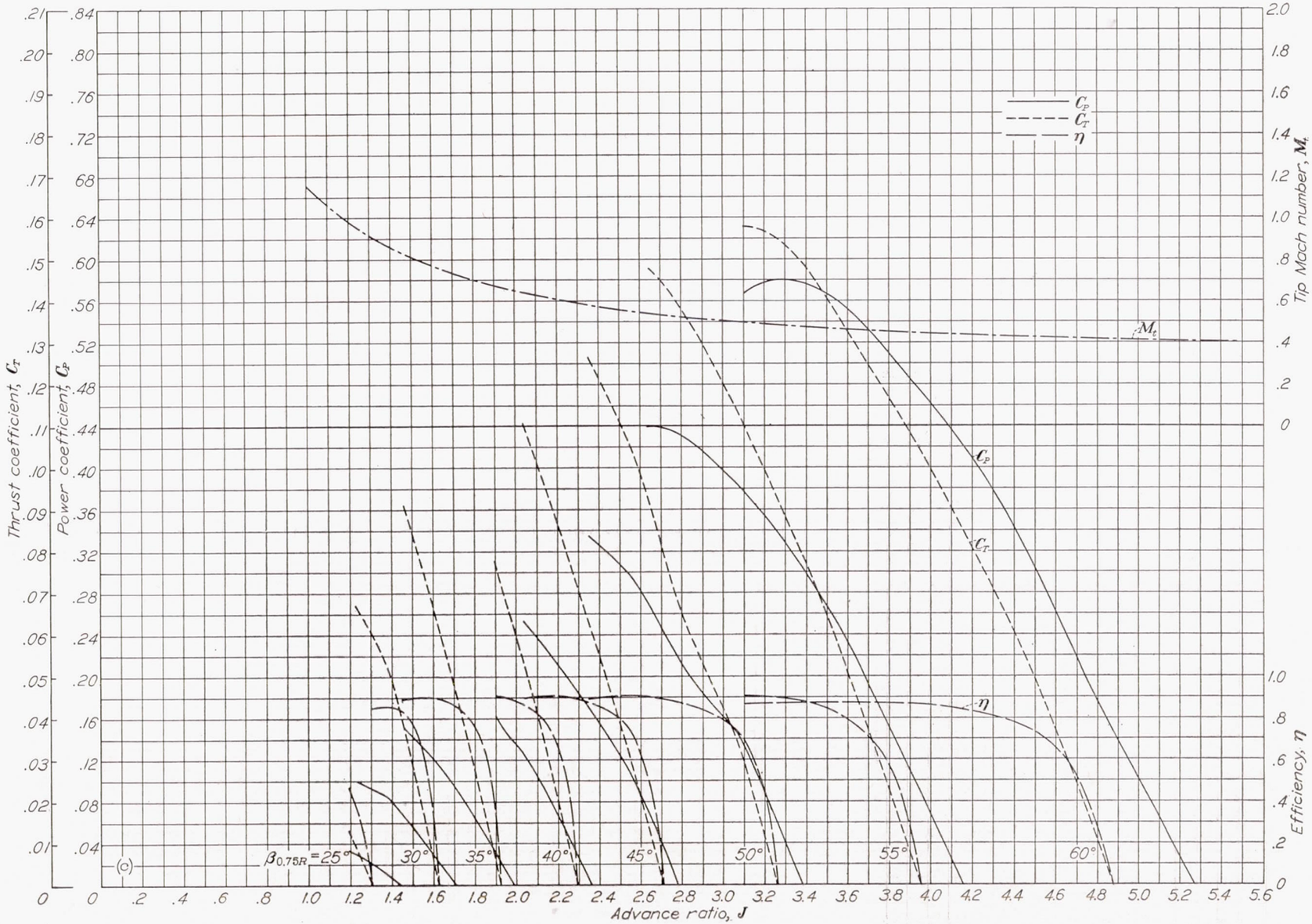
(a) M=0.165.

FIGURE 6.—Characteristics for the NACA 4-(10)(08)-03 propeller.



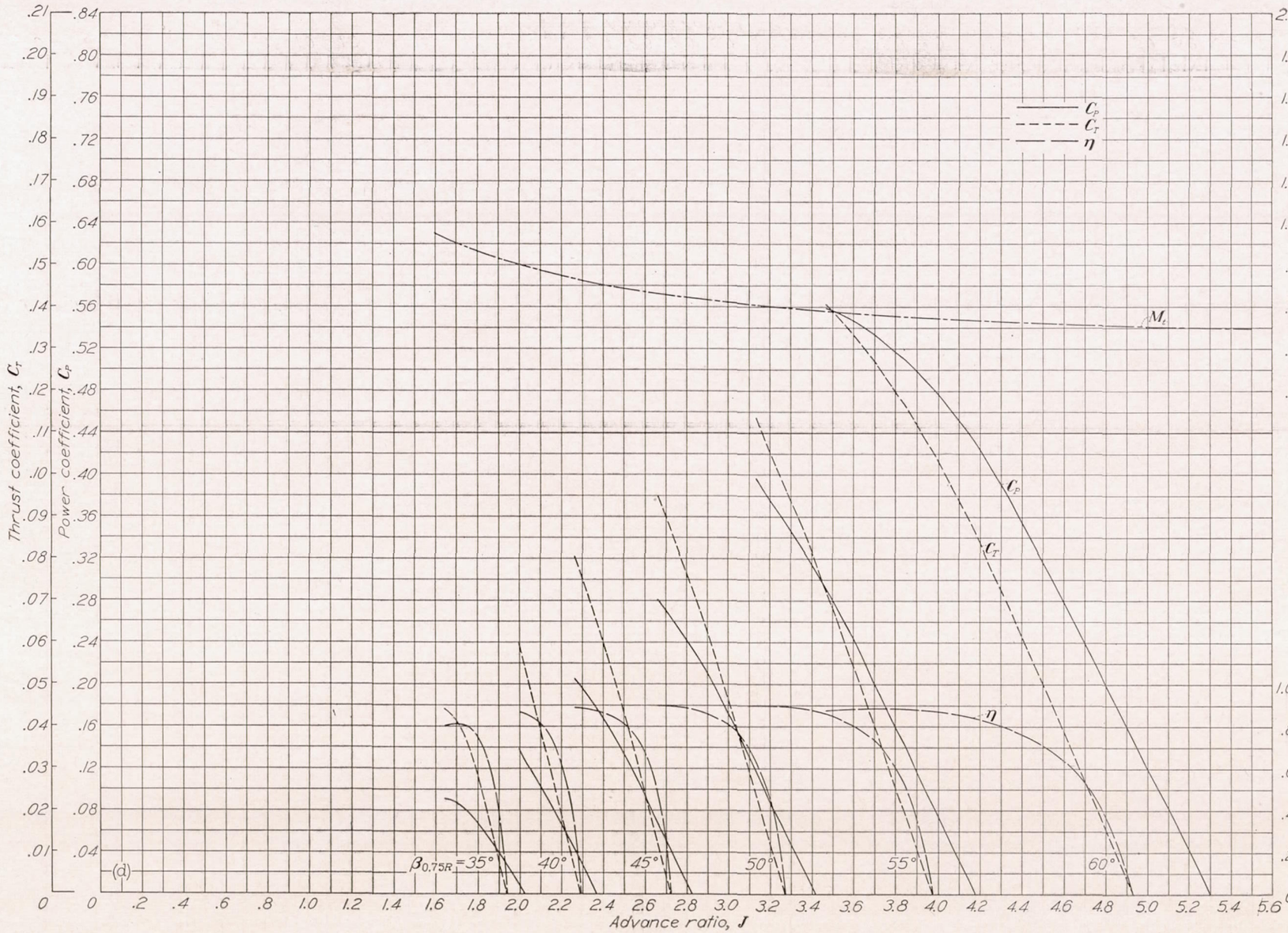
(b) $M=0.23$.

FIGURE 6.—Continued.



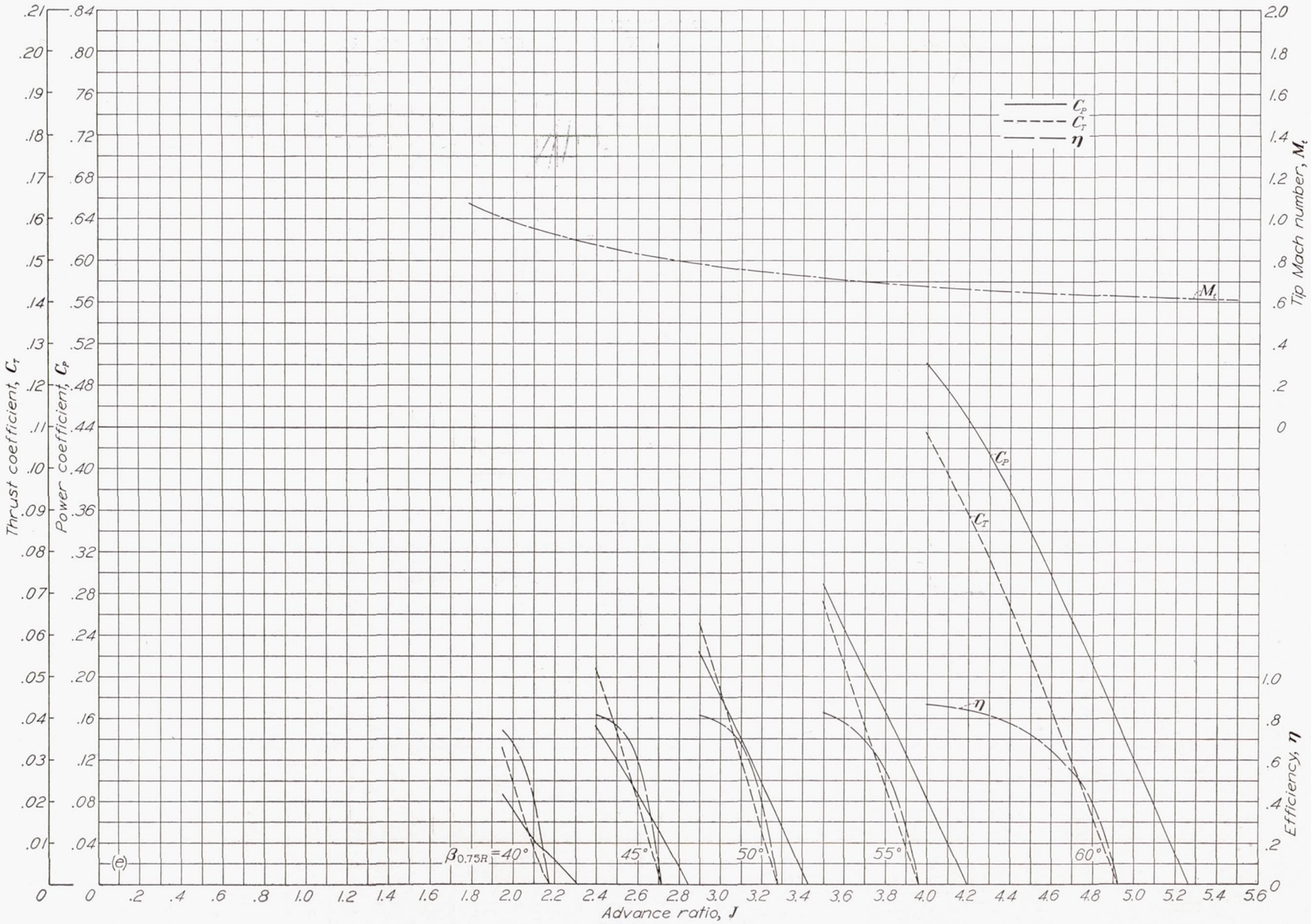
(c) M=0.35.

FIGURE 6.—Continued.



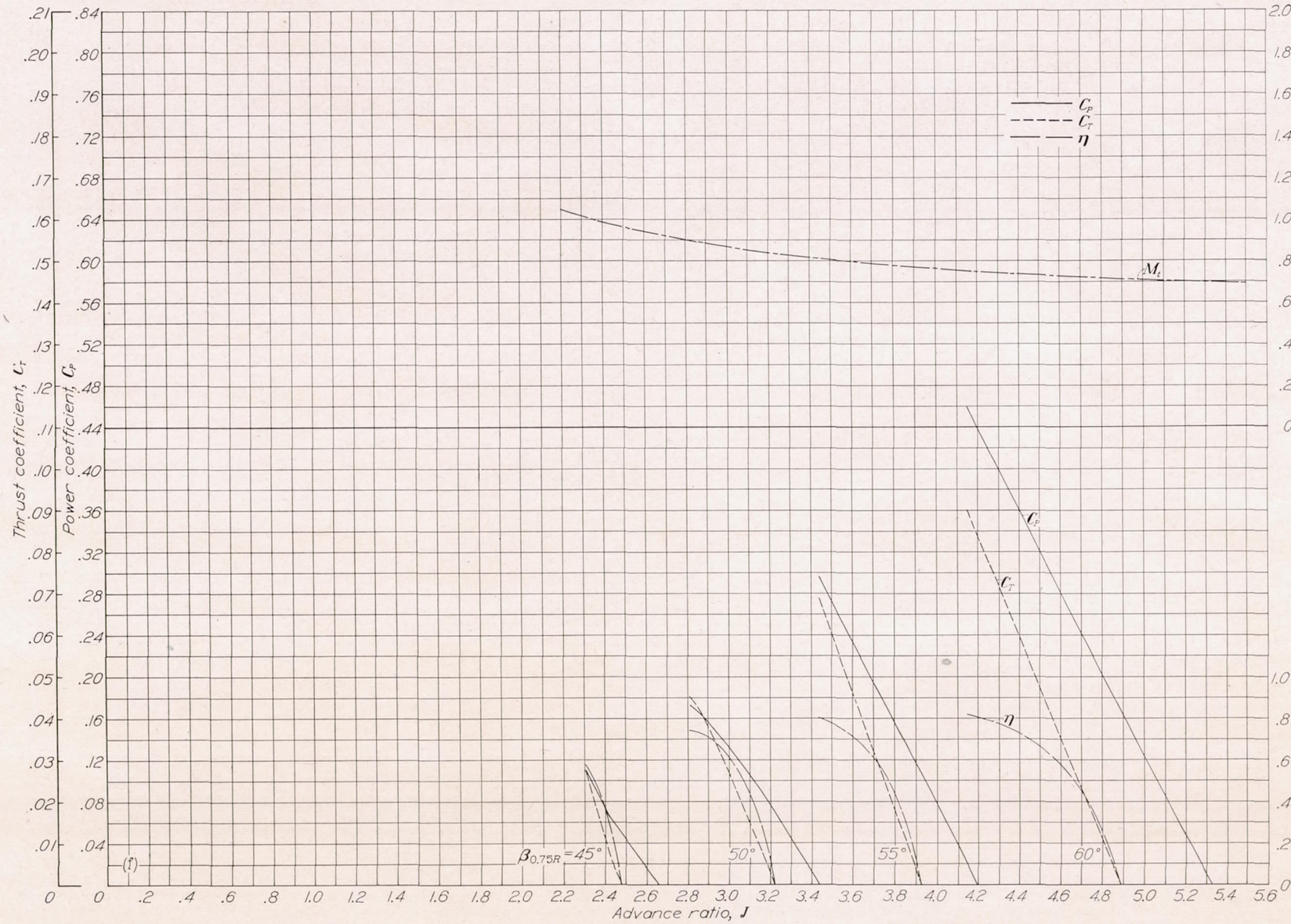
(d) M=0.43.

FIGURE 6.—Continued.



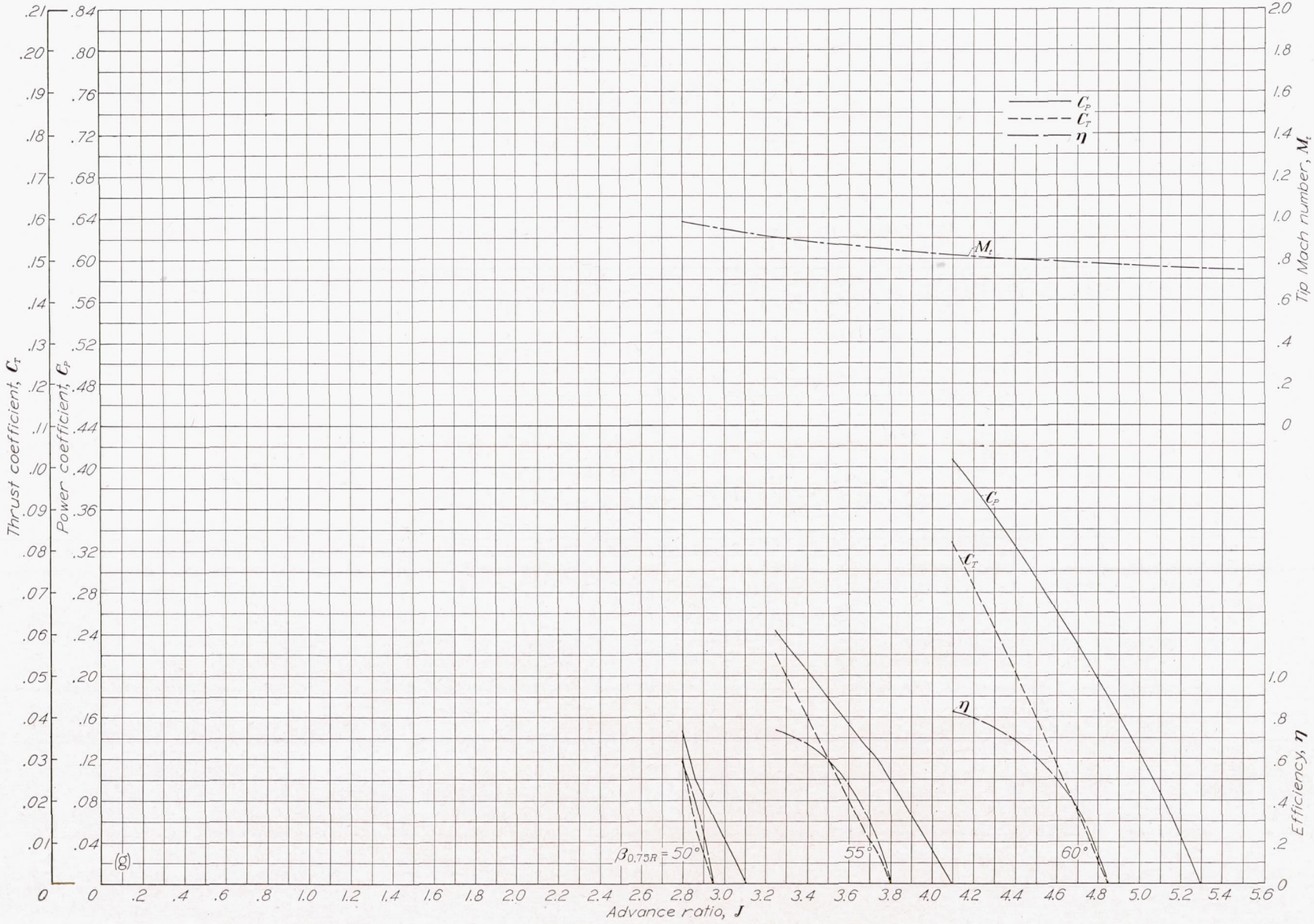
(e) M=0.53.

FIGURE 6.—Continued.



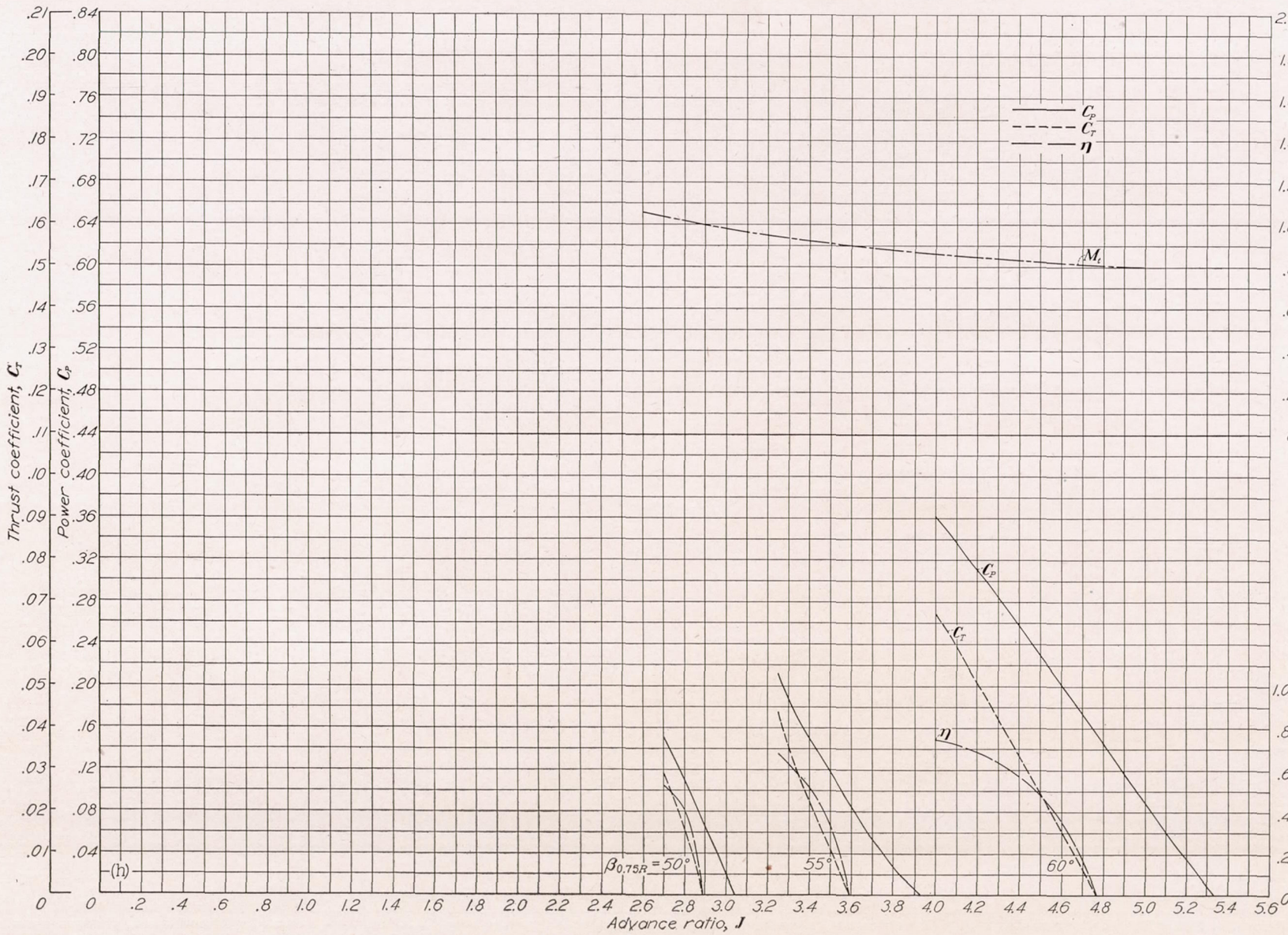
(f) $M=0.60$.

FIGURE 6.—Continued.



(g) $M=0.65$.

FIGURE 6.—Continued.



(h) $M=0.675$.

FIGURE 6.—Continued.

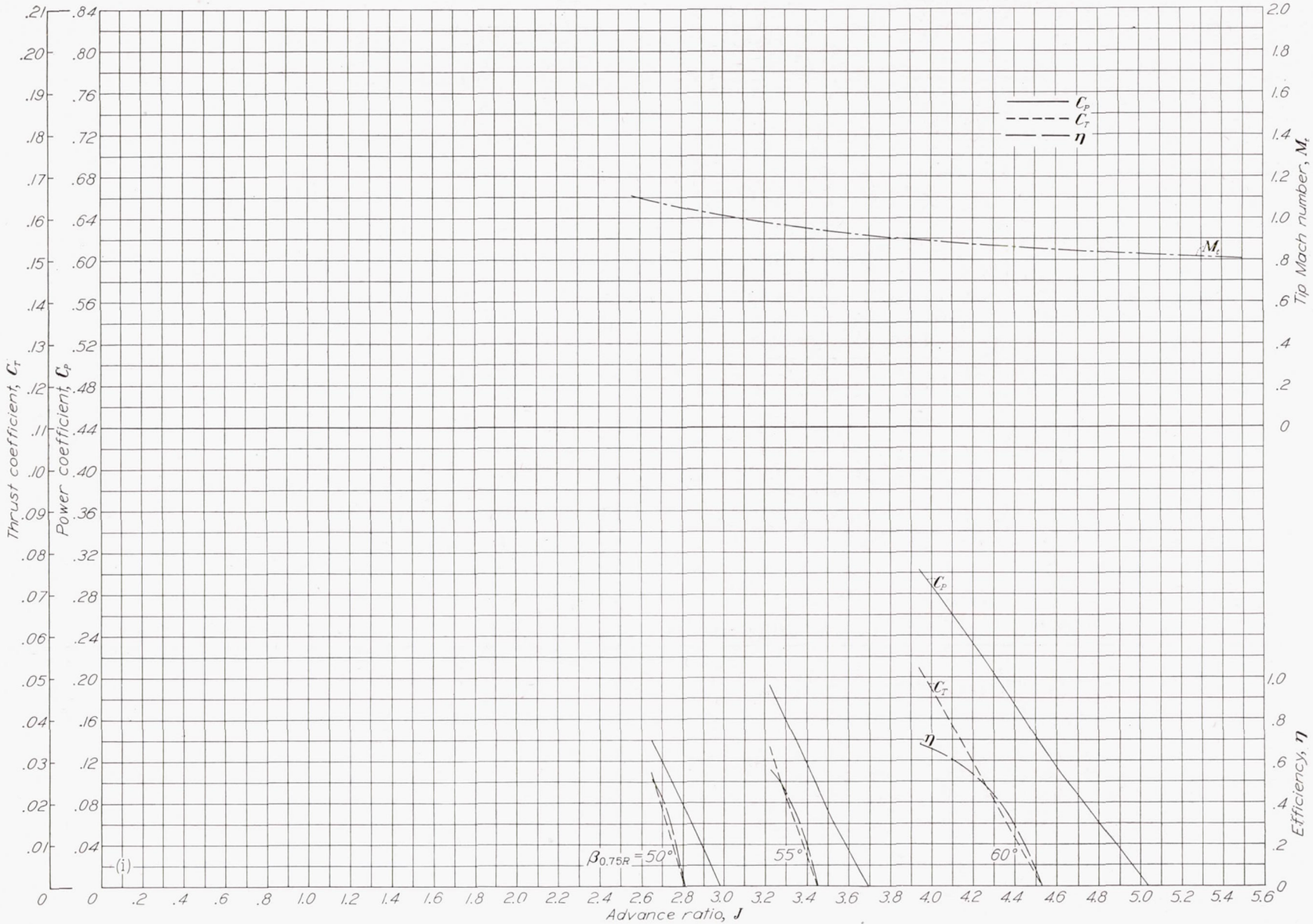
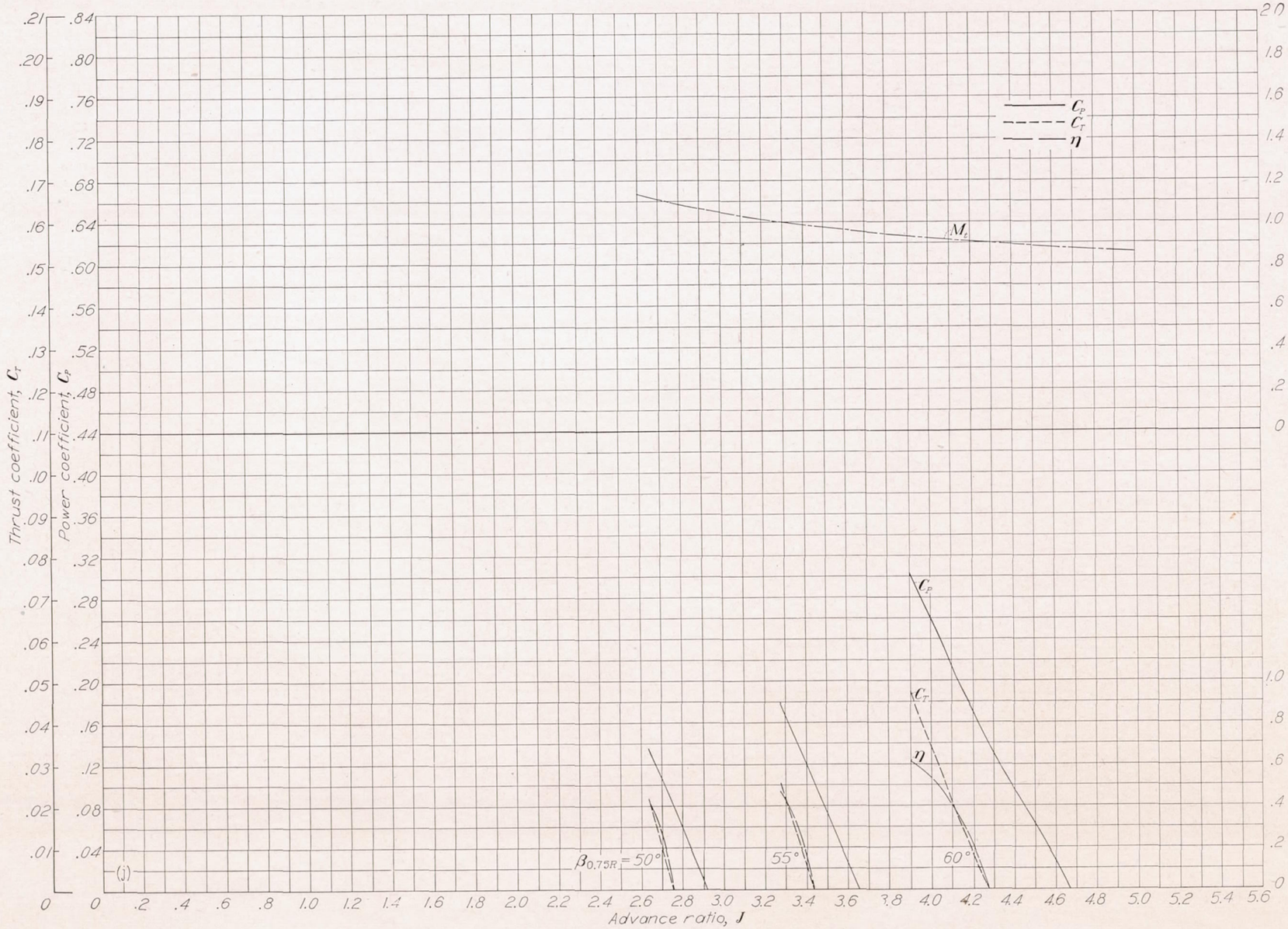


FIGURE 6.—Continued.



(j) $M=0.725$.

FIGURE 6.—Concluded.

Effect of camber on thrust coefficient.—The primary effect of using propeller blades of increased design camber (increased design lift coefficient) is to increase the power absorbed by the blades and consequently to increase the thrust. A typical illustration of the increase in thrust produced by increasing the design camber is shown in figure 7 in which the thrust coefficients for the high-camber, medium-camber, and low-camber propellers for a blade angle of 45° and a forward Mach number of 0.23 are compared. The power-coefficient curves are similar and hence are not shown. For cases in which take-off and climb performances are of prime importance, the increased thrust produced by the blades of high design camber may determine the design; greater thrusts may be produced with no increase in propeller weight. The maximum thrust coefficient and the thrust coefficient for maximum efficiency also increase with an increase in design camber, as shown in figures 8 and 9 for Mach

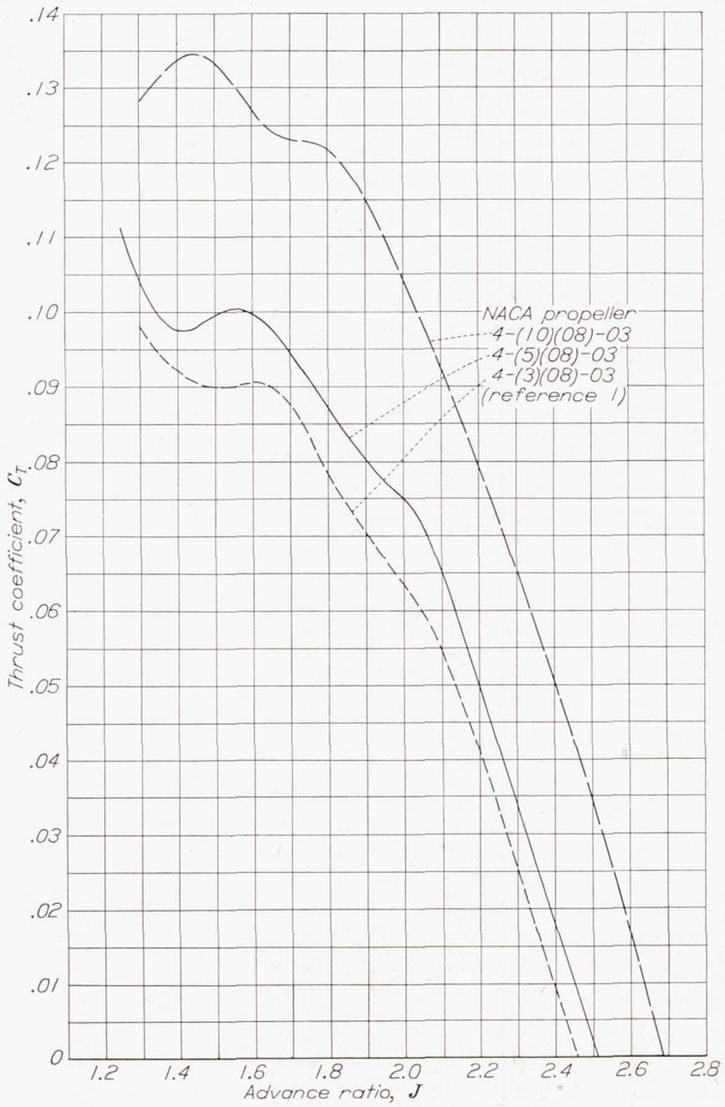


FIGURE 7.—Effect of design camber on thrust coefficient. $M=0.23$; $\beta_{0.75R}=45°$.

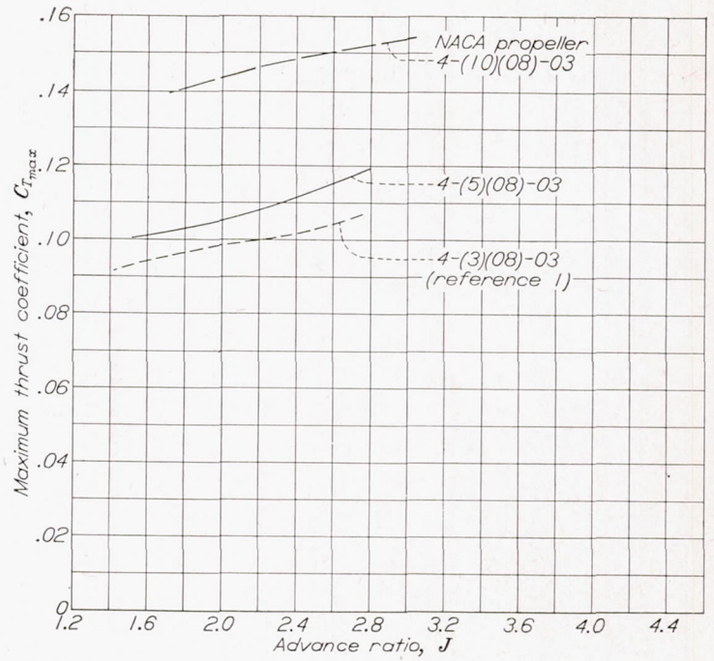


FIGURE 8.—Effect of design camber on maximum thrust coefficient. $M=0.165$.

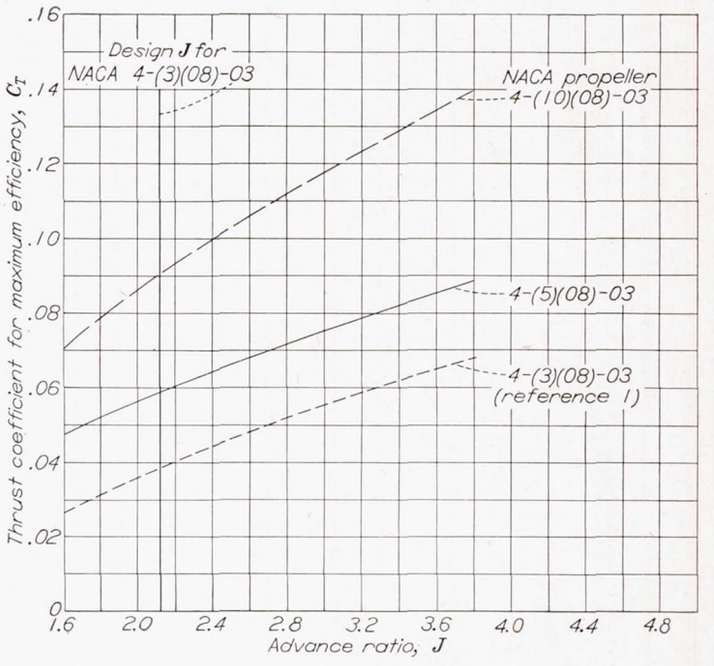


FIGURE 9.—Effect of design camber on thrust coefficient for maximum efficiency. $M=0.35$.

numbers of 0.165 and 0.35, respectively. The percentage of increase in thrust is less than the percentage of increase in corresponding design camber. The maximum thrust coefficients for the medium-camber propeller are 7 to 11 percent greater than for the low-camber propeller. The maximum thrust coefficients for the high-camber propeller are 41 to 46 percent greater than for the low-camber propeller. The increases in thrust coefficient for maximum efficiency are

much greater than the increase in maximum thrust coefficient. The thrust coefficients at maximum efficiency are 30 to 79 percent greater for the medium-camber propeller and 105 to 165 percent greater for the high-camber propeller than for the low-camber propeller.

Operation at high angles of attack may cause the blade sections to become stalled or nearly stalled so that the propeller efficiency is decreased because of increased profile-drag losses. The pressure distribution over these blade sections is therefore far from optimum and has high peaks that have a tendency to cause flow separation or to initiate compressibility shock. The use of blades of high design camber, however, makes it possible for the blade sections to operate at high section lift coefficients, which are obtained at angles of attack much lower than for blades of low design camber; thus, the tendency of the flow to separate is reduced and stalled conditions are largely eliminated. Since the pressure distribution about the sections may closely approximate the design distribution, the profile drag and the tendency for shock to be initiated are reduced.

Effect of camber and power loading on efficiency.—The effect of blade power loading on propeller efficiency for the high-camber, medium-camber, and low-camber propellers is shown in figure 10 for a forward Mach number of 0.165. Values of the power coefficient of about 0.10 for these propellers represent operation at high lift coefficients for values of the advance ratio corresponding to take-off and climb. For this condition, the propeller efficiency decreases very rapidly as the power coefficient is increased because of the increased profile-drag losses and the failure of the lift to increase beyond the maximum section lift coefficient with further increase of angle of attack. The ideal efficiency computed from the momentum theory is also shown in figure 10 for comparison. The divergence of the measured efficiency from the ideal efficiency emphasizes the magnitude of the profile-drag and induced losses.

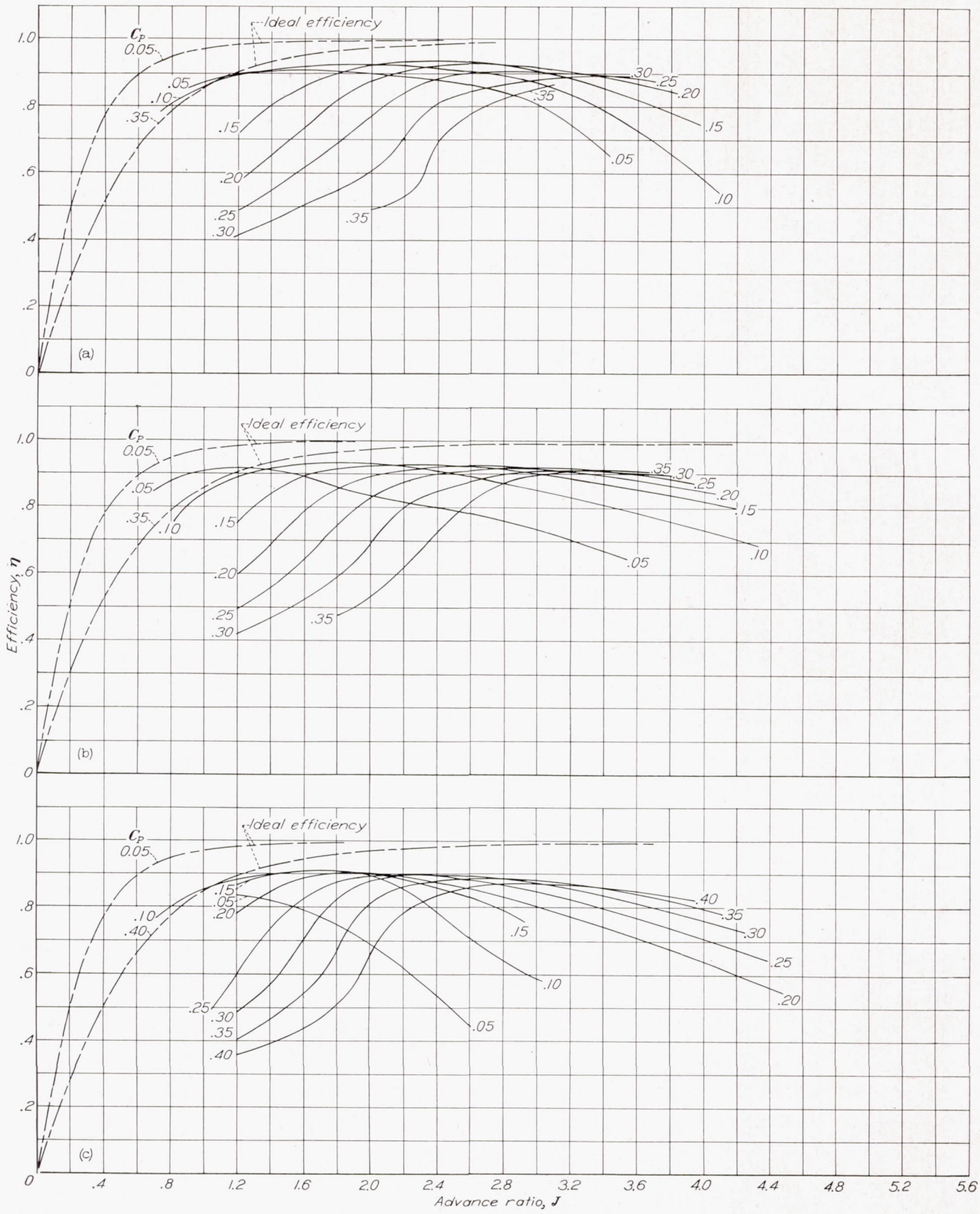
The effect of design camber for constant values of power coefficient is shown in figure 11 for a forward Mach number of 0.165. At low advance ratios corresponding to take-off and climb, increased camber gives increased efficiency at high power coefficients. At these high power coefficients, the high-camber blade is 15 to 25 percent more efficient than the low-camber and medium-camber blades. At low advance ratios and for low power coefficients, the high-camber blade is approximately 5 percent less efficient than the low-camber and medium-camber blades. These variations emphasize the necessity for choosing the correct blade camber to meet operational requirements. The high-camber blade is generally more efficient than the low-camber and medium-camber blades up to values of the advance ratio approximately 10 times the value of the power coefficient. The medium-camber blade is generally as much as 5 percent more efficient than the low-camber blade for the same operating range. These results suggest that a satisfactory compromise propeller may be designed by proper selection of the design camber.

Single-station analysis of camber effects.—In order to show the effect of design camber and operating lift coefficients on propeller section efficiency, the results of tests of the NACA 16-series airfoil sections of 9-percent thickness (reference 2) were chosen as representative of the section at the 0.7-radius station. Since this analysis is not an attempt to explain or present compressibility effects, data at a Mach number of 0.45 are used. It can be shown that the section efficiency is given by

$$\eta=\frac{\tan \phi_0}{\tan (\phi+\gamma)} \tag{1}$$

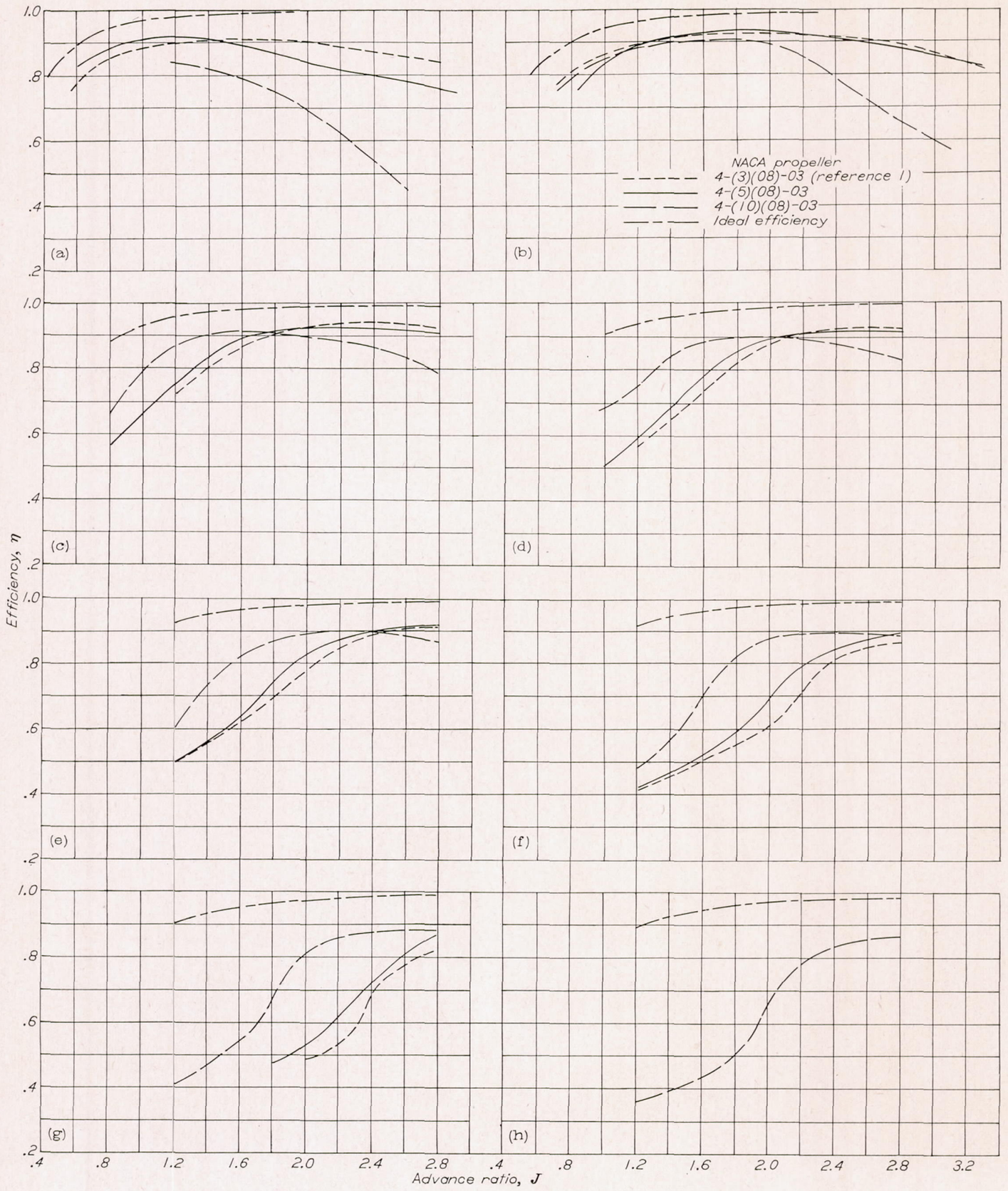
Figure 12 shows the results obtained by use of equation (1). For a given operating lift coefficient, the induced angle of attack for all the sections is the same; hence, the efficiency shows the effect of lift-drag ratio. The most obvious result is that the sections with design lift coefficients between 0.3 and 0.5 are the most efficient, because these sections have the highest lift-drag ratios at maximum efficiency. For sections with design lift coefficients of 0.3 and lower, the maximum efficiency occurs at operating lift coefficients greater than the design lift coefficients. For sections with design lift coefficients higher than 0.3, the maximum efficiency occurs at operating lift coefficients lower than the design lift coefficient. The maximum attainable efficiency at any blade operating lift coefficient is represented by the envelope of the efficiencies in figure 12. The greatest efficiency attainable for operation at a given lift coefficient occurs when the section has a design lift coefficient equal to the operating lift coefficient.

Effect of compressibility on maximum efficiency.—The envelope efficiencies for the high-camber, medium-camber, and low-camber propellers are presented in figure 13 for forward Mach numbers from 0.23 to 0.70. The values of advance ratio at which propeller tip Mach numbers of 0.9, 1.0, and 1.1 are reached are indicated by vertical dash lines labeled with the value of M_t. The medium-camber propeller gave the highest efficiencies for all advance ratios and for forward Mach numbers up to 0.53. In most cases, the medium-camber propeller was 2 to 5 percent more efficient than the low-camber propeller. The high-camber propeller gave peak efficiencies 3 to approximately 12 percent lower than those for the medium-camber propeller; the higher efficiency losses were due mainly to compressibility effects. At tip Mach numbers greater than approximately 0.90, the low-camber and medium-camber propellers showed compressibility losses. The high-camber propeller, however, showed an appreciable compressibility loss at a tip Mach number considerably below 0.90, but the efficiencies were still above 82 percent.



(a) NACA 4-(3)(08)-03 propeller (reference 1).
(b) NACA 4-(5)(08)-03 propeller.
(c) NACA 4-(10)(08)-03 propeller.

FIGURE 10.—Effect of power loading on efficiency. $M=0.165$.



(a) C_P=0.05.
(b) C_P=0.10.
(c) C_P=0.15.
(d) C_P=0.20.
(e) C_P=0.25.
(f) C_P=0.30.
(g) C_P=0.35.
(h) C_P=0.40.

FIGURE 11.—Effect of design camber and power loading on efficiency. M=0.165.

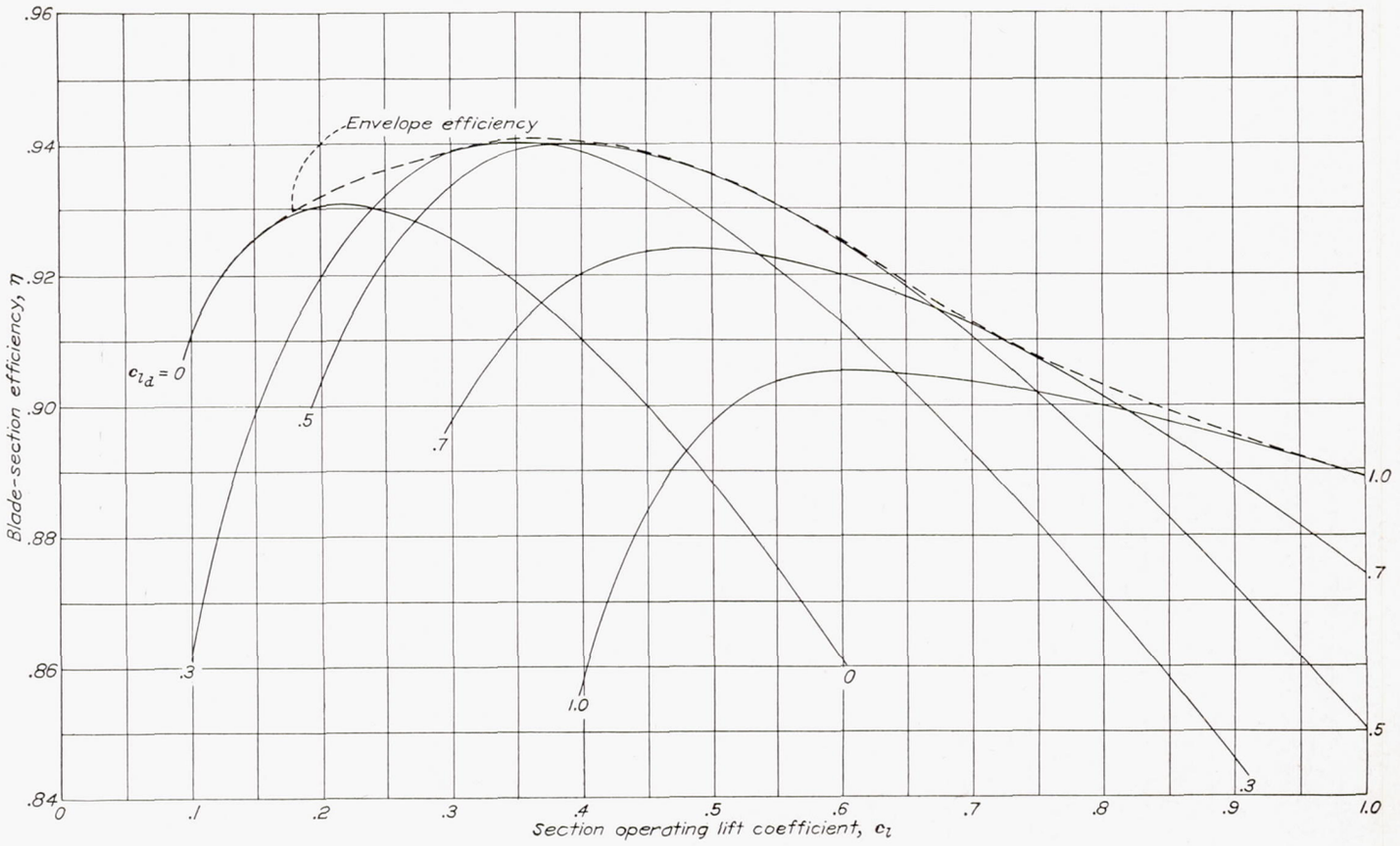
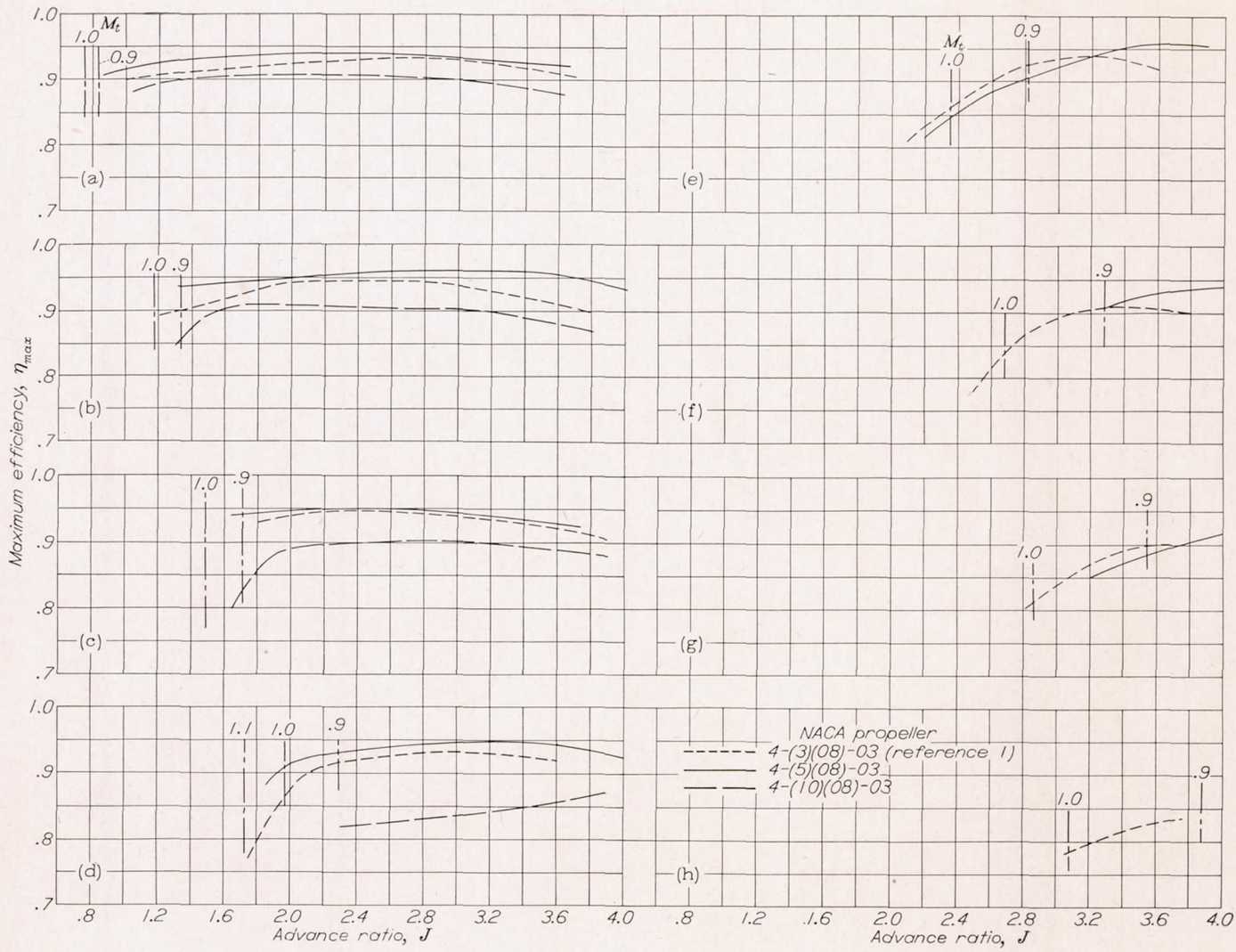


FIGURE 12.—Effect of design camber on blade-section efficiency, from single-station analysis using NACA 16-series sections. $\frac{r}{R}$=0.7; $\frac{h}{b}$=0.09; ϕ=44°; M=0.45.

The effect of compressibility on maximum efficiency is shown in figure 14 for a blade angle of 45°. Maximum efficiency differed very little for the low-camber and medium-camber propellers with critical tip Mach numbers of approximately 0.90 and 0.91, respectively. The high-camber propeller begins to show compressibility losses at a tip Mach number of 0.70, but the rate of loss is less than that for the low-camber and medium-camber propellers. The low critical speed of the propeller with the highest camber obviously excludes the use of this propeller for very efficient high-speed operation. The early compressibility losses for the high-camber propeller are due, in part at least, to the high power absorbed. If the low-camber and medium-camber propellers absorbed the same power as the high-camber propeller, these propellers would have to operate at high angles of attack; this operation would produce high pressure peaks and perhaps earlier and more extensive compressibility losses.

In order for the low-camber and medium-camber propellers to absorb the same power as the high-camber propeller and still operate at high efficiencies, a considerable increase in solidity would be necessary. The large power-absorbing capacity of the high-camber propeller, however, makes it useful for conditions of operation at which large values of thrust are required, even at high speeds. For example, the influence of design camber on maximum efficiency and on the power absorbed at maximum efficiency is presented in figure 15 for an advance ratio of 2.48 at forward Mach numbers of 0.23 and 0.53 (tip Mach numbers of 0.37 and 0.86, respectively). For these conditions, the high-camber propeller shows a compressibility loss of 8 percent. The high-camber propeller absorbs 55 percent more power than the medium-camber propeller and 75 percent more power than the low-camber propeller at a forward Mach number of 0.53. The corresponding differences in efficiency are reductions of 9 and 10 percent, which result in net thrust increases of 46 and 65 percent, respectively, for the high-camber propeller; in addition, these increases in thrust are obtained with no increase in propeller weight.

Effect of compressibility and power disk loading on maximum efficiency.—The effects of power disk-loading coefficient P_c and compressibility on maximum efficiency are shown in figure 16. The curve for the ideal efficiency obtained from axial-momentum considerations is also shown. The ideal efficiency deviates from 100 percent solely because of the induced loss due to increasing the axial velocity of the air in the slipstream. The additional losses for an actual propeller, however, are due to profile-drag and rotational induced losses. The induced losses for these propellers are small, and the differences shown between the ideal and the measured efficiencies are principally due to blade drag loss. At a given value of the forward Mach number, increased values of P_c correspond to loadings at low values of the advance ratio.



(a) M=0.23.
(b) M=0.35.
(c) M=0.43.
(d) M=0.53.
(e) M=0.60.
(f) M=0.65.
(g) M=0.675.
(h) M=0.70.

FIGURE 13.—Effect of design camber and compressibility on envelope efficiency.

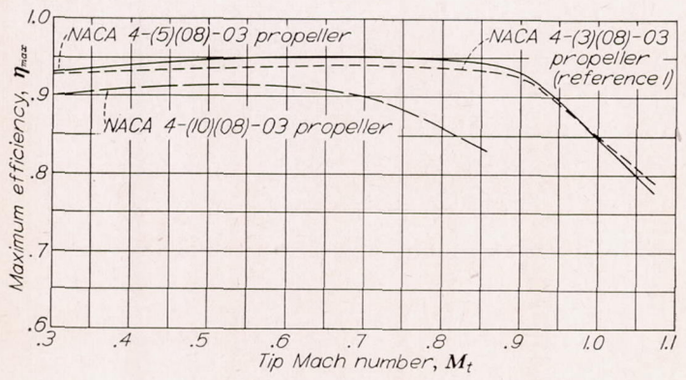


FIGURE 14.—Effect of compressibility on maximum efficiency. $\beta_{0.75R}$=45°.

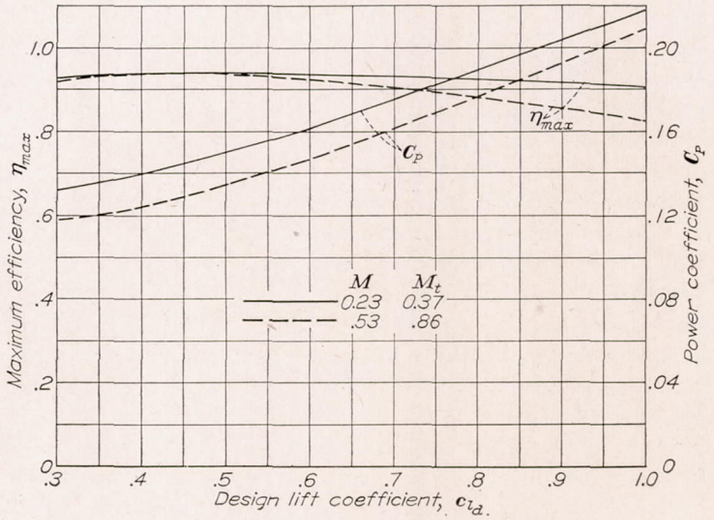
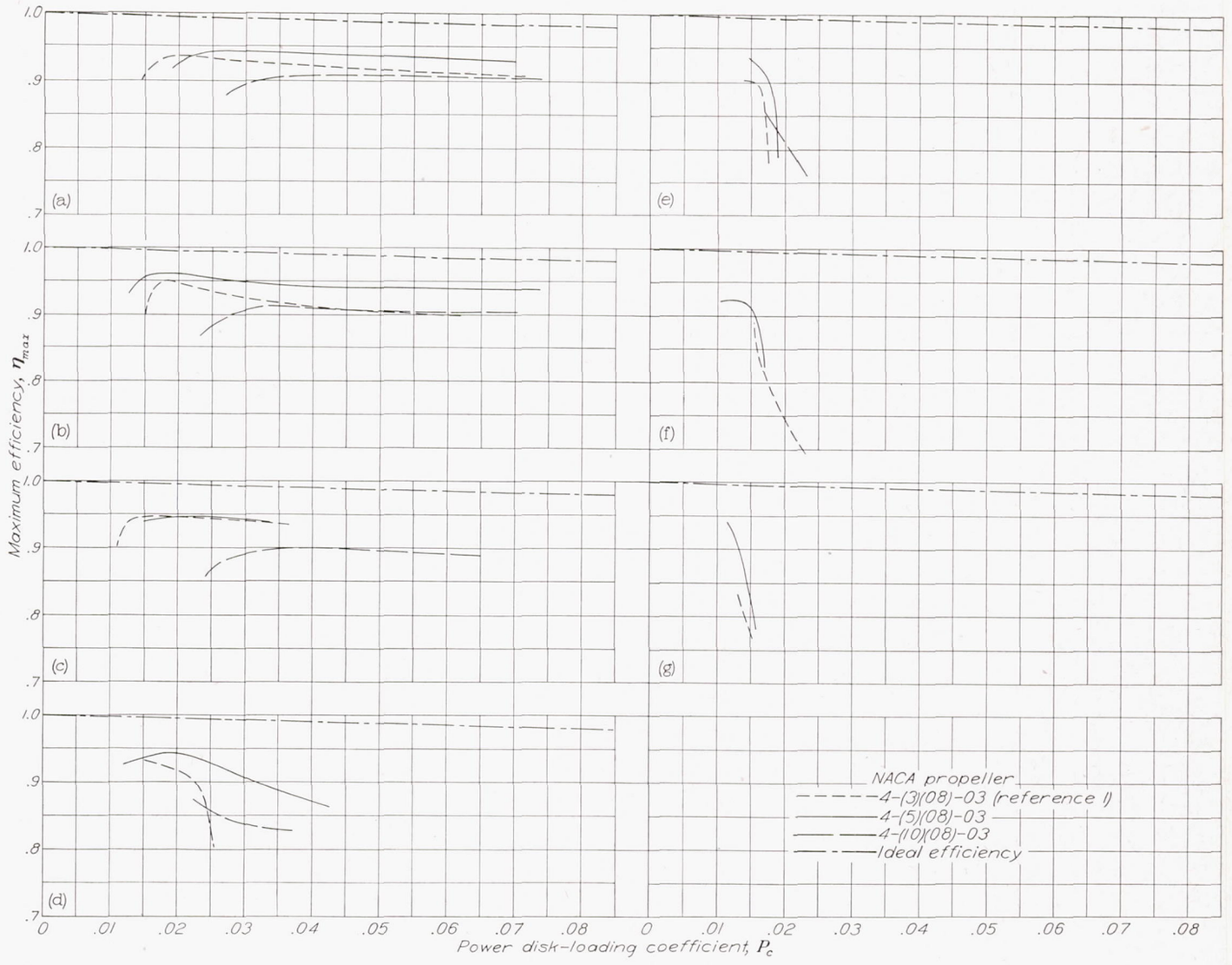


FIGURE 15.—Effect of blade-section design lift coefficient on maximum efficiency and power absorbed at maximum efficiency. J=2.48.



(a) M=0.23.
(b) M=0.35.
(c) M=0.43.
(d) M=0.53.
(e) M=0.65.
(f) M=0.675.
(g) M=0.70.

FIGURE 16.—Effect of power disk loading and compressibility on maximum efficiency.

At low values of the forward Mach number (fig. 16 (a)), for example, the maximum-efficiency curves for the three propellers are parallel for high values of P_c and are relatively close to the ideal-efficiency curve. This agreement is expected, because these propellers have approximately the optimum pitch distributions for these values of P_c and because the profile-drag and induced losses are not expected to change very much. Since at a constant forward Mach number the high values of P_c for each curve correspond to operation at the highest tip speeds for that condition, compressibility losses would appear at the high values of the power disk-loading coefficient. No compressibility losses appear for the low forward Mach numbers. For all propellers, large losses begin to appear at a forward Mach number of 0.53 and are most severe for the low-camber propeller and least severe for the medium-camber propeller. At a Mach number of 0.65, the high-camber propeller appears to be more efficient than the other propellers for operation at the high power disk-loading coefficients. Of particular interest is the greatly reduced range of power disk-loading coefficient for which the maximum efficiencies obtained at low Mach numbers can be maintained at high forward Mach numbers. Similar results are shown in reference 1. At forward Mach numbers of 0.53 or greater, the range of power disk-loading coefficient that gives high efficiencies for the low-camber propeller is greatly reduced because of compressibility losses. Previous results (reference 1) have indicated that the range of power disk-loading coefficient for high efficiency may be selected by change of blade solidity. The results reported herein also indicate that the same effect can be produced by

change of camber. This effect is particularly pronounced for forward Mach numbers of 0.53 and 0.65 (figs. 16 (d) and 16 (e)). The medium-camber and high-camber propellers can operate more efficiently at high values of the power disk-loading coefficient, but compressibility effects have considerably lowered the efficiencies. Changing the design camber thus offers another possibility of operating at high power disk loadings without too much loss in maximum efficiency.

The power disk-loading coefficient for which low-speed efficiencies may be maintained at high speeds can also be increased by using a greater number of similar blades, as was pointed out in reference 1. For operation at very high speeds, particular consideration must therefore be given to the aerodynamic design. The design of a propeller then approaches the design for a specific condition of operation to obtain high efficiencies because of the reduced range of available power disk loading.

CONCLUSIONS

Two-blade propellers designated the NACA 4–(5)(08)–03 (medium camber) and the NACA 4–(10)(08)–03 (high camber) propellers have been investigated in the Langley 8-foot high-speed tunnel through a range of blade angles from 20° to 60° for forward Mach numbers from 0.165 to 0.70 to determine the effect of camber and compressibility on propeller characteristics. The results of these tests and comparisons with results obtained from previous tests of the NACA 4–(3)(08)–03 (low camber) propeller indicated the following conclusions:

1. Propellers of high design camber were more efficient than propellers of low design camber for operation at high power coefficients. The propeller of highest camber gave efficiencies 15 to 25 percent greater than the efficiencies of the low-camber and medium-camber propellers for high power coefficients at advance ratios corresponding to take-off and climb at low Mach numbers.

2. The medium-camber propeller generally gave peak efficiencies 2 to 5 percent higher than the low-camber propeller and 3 to approximately 12 percent higher than the high-camber propeller. The high-camber propeller was operating at much higher power coefficients, which led to early compressibility effects.

3. The critical tip Mach number for maximum efficiency at the design blade angle of 45° was 0.01 higher for the medium-camber propeller than that for the low-camber propeller, which began to show compressibility losses at a tip Mach number of approximately 0.90. The high-camber propeller, which was operating at higher power coefficients than the other propellers, showed the largest compressibility losses. The compressibility losses for the high-camber propeller began at a tip Mach number as low as 0.70 but efficiencies of more than 82 percent were still maintained.

4. For a forward Mach number of 0.53 and an advance ratio of 2.48 (tip Mach number of 0.86), the high-camber propeller showed a compressibility loss of 8 percent in maximum efficiency but, because of the large power-absorbing capacity of this propeller, produced about 65 percent more thrust than the low-camber propeller and 46 percent more thrust than the medium-camber propeller.

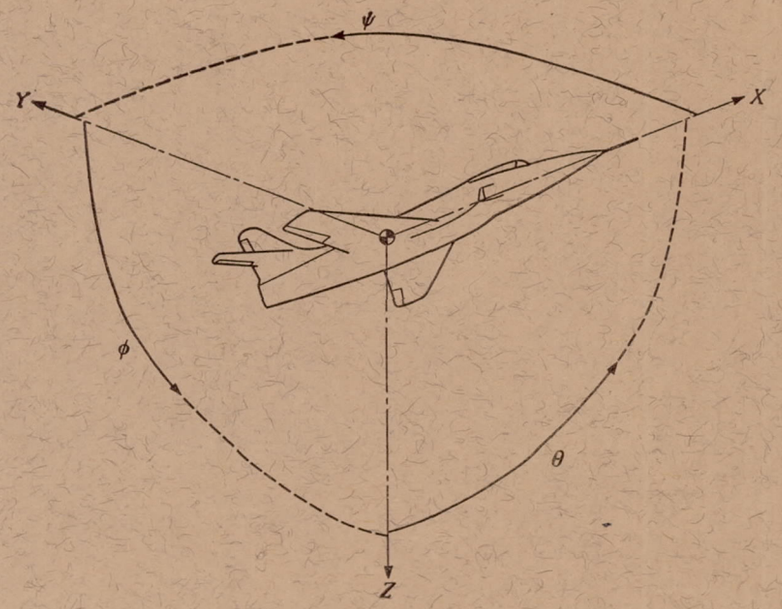
5. The range of power disk-loading coefficient over which high efficiencies could be obtained was greatly reduced at high speeds.

LANGLEY MEMORIAL AERONAUTICAL LABORATORY,
NATIONAL ADVISORY COMMITTEE FOR AERONAUTICS,
LANGLEY FIELD, VA., *May 7, 1945.*

REFERENCES

1. Stack, John, Draley, Eugene C., Delano, James B., and Feldman, Lewis: Investigation of the NACA 4–(3)(08)–03 and NACA 4–(3)(08)–045 Two-Blade Propellers at Forward Mach Numbers to 0.725 to Determine the Effects of Compressibility and Solidity on Performance. NACA Rep. 999, 1950.
2. Stack, John: Tests of Airfoils Designed to Delay the Compressibility Burble. NACA Rep. 763, 1943.
3. Hartman, Edwin P., and Feldman, Lewis: Aerodynamic Problems in the Design of Efficient Propellers. NACA ACR, Aug. 1942.

U. S. GOVERNMENT PRINTING OFFICE: 1951



Positive directions of axes and angles (forces and moments) are shown by arrows

Axis		Force (parallel to axis) symbol	Moment about axis			Angle		Velocities	
Designation	Symbol		Designation	Symbol	Positive direction	Designation	Symbol	Linear (component along axis)	Angular
Longitudinal	X	X	Rolling	L	$Y \longrightarrow Z$	Roll	ϕ	u	p
Lateral	Y	Y	Pitching	M	$Z \longrightarrow X$	Pitch	θ	v	q
Normal	Z	Z	Yawing	N	$X \longrightarrow Y$	Yaw	ψ	w	r

Absolute coefficients of moment

$C_l = \frac{L}{qbS}$ (rolling) $\quad C_m = \frac{M}{qcS}$ (pitching) $\quad C_n = \frac{N}{qbS}$ (yawing)

Angle of set of control surface (relative to neutral position), δ. (Indicate surface by proper subscript.)

4. PROPELLER SYMBOLS

D Diameter

p Geometric pitch

p/D Pitch ratio

V' Inflow velocity

V_s Slipstream velocity

T Thrust, absolute coefficient $C_T = \frac{T}{\rho n^2 D^4}$

Q Torque, absolute coefficient $C_Q = \frac{Q}{\rho n^2 D^5}$

P Power, absolute coefficient $C_P = \frac{P}{\rho n^3 D^5}$

C_s Speed-power coefficient $= \sqrt[5]{\frac{\rho V^5}{P n^2}}$

η Efficiency

n Revolutions per second, rps

Φ Effective helix angle $= \tan^{-1}\left(\frac{V}{2\pi r n}\right)$

5. NUMERICAL RELATIONS

1 hp=76.04 kg-m/s=550 ft-lb/sec

1 metric horsepower=0.9863 hp

1 mph=0.4470 mps

1 mps=2.2369 mph

1 lb=0.4536 kg

1 kg=2.2046 lb

1 mi=1,609.35 m=5,280 ft

1 m=3.2808 ft